

*J. Math. Biol. 700 (116)*  
**OFFICIAL ORGAN OF THE RADIATION RESEARCH SOCIETY**

# **RADIATION RESEARCH**

**EDITOR-IN-CHIEF: R. J. M. FRY**

**Volume 116, 1988**



**ACADEMIC PRESS, INC.**

San Diego New York Boston  
London Sydney Tokyo Toronto



Copyright © 1988 by Academic Press, Inc.

All rights reserved

No part of this publication may be reproduced or transmitted in any form or by any means, electronic or mechanical, including photocopy, recording, or any information storage and retrieval system, without permission in writing from the copyright owner.

The appearance of the code at the bottom of the first page of an article in this journal indicates the copyright owner's consent that copies of the article may be made for personal or internal use, or for the personal or internal use of specific clients. This consent is given on the condition, however, that the copier pay the stated per copy fee through the Copyright Clearance Center, Inc. (27 Congress Street, Salem, Massachusetts 01970), for copying beyond that permitted by Sections 107 or 108 of the U. S. Copyright Law. This consent does not extend to other kinds of copying, such as copying for general distribution, for advertising or promotional purposes, for creating new collective works, or for resale. Copy fees for pre-1988 articles are as shown on the article title pages; if no fee code appears on the title page, the copy fee is the same as for current articles.

0033-7587/88 \$3.00

MADE IN THE UNITED STATES OF AMERICA



# RADIATION RESEARCH

---

OFFICIAL ORGAN OF THE RADIATION RESEARCH SOCIETY

---

*Editor-in-Chief:* R. J. M. FRY, Biology Division, Oak Ridge National Laboratory, P.O. Box 2009, Oak Ridge, Tennessee 37831-8077

*Managing Editor:* MARTHA EDINGTON, University of Tennessee–Oak Ridge Graduate School of Biomedical Sciences, Biology Division, Oak Ridge National Laboratory, P.O. Box 2009, Oak Ridge, Tennessee 37831-8077

## ASSOCIATE EDITORS

G. E. ADAMS, Medical Research Council,  
Harwell, Didcot, Oxfordshire, England

K. K. ANG, University of Texas

J. S. BEDFORD, Colorado State University

C. A. CAIN, University of Illinois

J. DENEKAMP, Gray Laboratory,  
Northwood, Middlesex, England

W. C. DEWEY, University of California, San  
Francisco

R. E. DURAND, British Columbia Cancer  
Research Center, Vancouver, Canada

E. R. EPP, Massachusetts General Hospital

C. R. GEARD, Columbia University

E. L. GILLETTE, Colorado State University

D. J. GRDINA, Argonne National Laboratory

R. N. HAMM, Oak Ridge National Laboratory

F. W. HETZEL, Henry Ford Hospital and  
Oakland University

M. Z. HOFFMAN, Boston University

L. E. HOPWOOD, Medical College of  
Wisconsin

R. E. KRISCH, University of Pennsylvania

J. B. MITCHELL, National Cancer Institute

J. L. REDPATH, University of California, Irvine

M. A. J. RODGERS, Bowling Green State  
University

W. SCHIMMERLING, Lawrence Berkeley  
Laboratory

W. U. SHIPLEY, Massachusetts General  
Hospital

E. L. TRAVIS, University of Texas

R. L. ULLRICH, University of Texas

R. R. WEICHSELBAUM, University of Chicago

## OFFICERS OF THE SOCIETY

*President:* GEORGE M. HAHN, Department of Radiology, Stanford University School of Medicine, Stanford, California 94305

*Vice President and President-Elect:* JOEL S. BEDFORD, Department of Radiology and Radiation Biology, Colorado State University, Fort Collins, Colorado 80523

*Secretary-Treasurer:* E. JOHN AINSWORTH, Lawrence Berkeley Laboratory, University of California, Berkeley, California 94720

*Editor-in-Chief:* R. J. M. FRY, Biology Division, Oak Ridge National Laboratory, P.O. Box 2009, Oak Ridge, Tennessee 37831-8077

*Administrative Director:* MEG KEISER, 1101 Market Street—14th Floor, Philadelphia, Pennsylvania 19107

## ANNUAL MEETING

1989: March 19–23, Seattle, Washington

Titus C. Evans, Editor-in-Chief Volumes 1–50  
Oddvar F. Nygaard, Editor-in-Chief Volumes 51–79  
Daniel Billen, Editor-in-Chief Volumes 80–113



Councilors, Radiation Research Society 1988–1989

PHYSICS

G. C. Li, University of California, San Francisco

R. W. Wood, Department of Energy

BIOLOGY

R. E. Durand, British Columbia Cancer Reserch Centre,  
Vancouver, Canada

S. S. Wallace, University of Vermont

MEDICINE

E. L. Gillette, Colorado State University

R. C. Urtasun, University of Alberta, Canada

CHEMISTRY

J. A. Raleigh, University of North Carolina

J. L. Redpath, University of California, Irvine

AT-LARGE

H. H. Evans, Case Western Reserve University

J. E. Moulder, Medical College of Wisconsin

# CONTENTS OF VOLUME 116

NUMBER 1, OCTOBER 1988

R. J. M. FRY. Editorial .....	1
JOHN D. BOICE, JR., GÖRAN ENGHOLM, RUTH A. KLEINERMAN, MARIA BLETNER, MARILYN STOVALL, HERMANN LISCO, WILLIAM C. MOLONEY, DONALD F. AUSTIN, ANTONIO BOSCH, DIANE L. COOKFAIR, EDWARD T. KREMENTZ, HOWARD B. LATOURETTE, JAMES A. MERRILL, LESTER J. PETERS, MILFORD D. SCHULZ, HANS H. STORM, ELISABETH BJÖRKHOLM, FOLKE PETTERSSON, C. M. JANINE BELL, MICHEL P. COLEMAN, PATRICIA FRASER, FRANK E. NEAL, PATRICIA PRIOR, N. WON CHOI, T. GREGORY HISLOP, MARIA KOCH, NANCY KREIGER, DOROTHY ROBB, DIANE ROBSON, D. H. THOMSON, H. LOCHMÜLLER, DIETRICH VON FOURNIER, ROLF FRISCHKORN, KJELL E. KJØRSTAD, ARJA RIMPELA, MARIE-HÉLÈNE PEJOVIC, VERA POMPE KIRN, HANNA STANKUSOVA, FRANCO BERRINO, KRISTJAN SIGURDSSON, GEORGE B. HUTCHISON, AND BRIAN MACMAHON. Radiation Dose and Second Cancer Risk in Patients Treated for Cancer of the Cervix .....	3
TAKASHI KONDO, C. MURALI KRISHNA, AND PETER RIESZ. Sonolysis, Radiolysis, and Hydrogen Peroxide Photolysis of Pyrimidine Derivatives in Aqueous Solutions: A Spin-Trapping Study .....	56
B. FERTIL, P. J. DESCHAVANNE, D. DEBIEU, AND E. P. MALAISE. Correlation between PLD Repair Capacity and the Survival Curve of Human Fibroblasts in Exponential Growth Phase: Analysis in Terms of Several Parameters .....	74
LIANG-YAN XUE, LIBBY R. FRIEDMAN, AND NANCY L. OLEINICK. Repair of Chromatin Damage in Glutathione-Depleted V-79 Cells: Comparison of Oxidic and Hypoxic Conditions .....	89
SARA ROCKWELL, SUSAN R. KEYES, AND ALAN C. SARTORELLI. Preclinical Studies of Porfomycin as an Adjunct to Radiotherapy .....	100
HARM H. KAMPINGA, WILLIAM D. WRIGHT, ANTONIUS W. T. KONINGS, AND JOSEPH L. ROTI ROTI. The Interaction of Heat and Radiation Affecting the Ability of Nuclear DNA to Undergo Supercoiling Changes .....	114
VICRAM GUPTA AND JAMES A. BELLI. Enhancement of Radiation Sensitivity by Postirradiation Hypoxia: Time Course and Oxygen Concentration Dependency .....	124
RAPHAEL GORODETSKY, WILLIAM H. MCBRIDE, AND H. RODNEY WITHERS. Assay of Radiation Effects in Mouse Skin as Expressed in Wound Healing .....	135
RENATO G. PANIZZON, WAYNE R. HANSON, DAVID E. SCHWARTZ, AND FREDERICK D. MALKINSON. Ionizing Radiation Induces Early, Sustained Increases in Collagen Biosynthesis: A 48-Week Study in Mouse Skin and Skin Fibroblast Cultures .....	145
CHARLES A. VIDAIR AND WILLIAM C. DEWEY. Two Distinct Modes of Hyperthermic Cell Death ..	157
LETTERS TO THE EDITOR	
D. J. BRENNER. Comments on "It Is Time to Reopen the Question of Thresholds in Radiation Exposure Responses" by J. R. Totter [ <i>Radiat. Res.</i> <b>114</b> , 1-2 (1988)] .....	172
WILLIAM H. ELLETT. The BEIR IV Report .....	173
BOOK REVIEWS	
J. F. FOWLER. <i>Radiobiology for the Radiologist</i> , 3rd ed., by Eric J. Hall .....	175
M. L. GRIEM. <i>Innovations in Radiation Oncology</i> , edited by H. Rodney Withers and Lester J. Peters .....	176
IN MEMORIAM	
PETER HERRLICH. Karl Günther Zimmer (1911-1988) .....	178
ANNOUNCEMENT .....	181

NUMBER 2, NOVEMBER 1988

N. F. METTING, H. H. ROSSI, L. A. BRABY, P. J. KLIUGA, J. HOWARD, M. ZAIDER, W. SCHIMMERLING, M. WONG, AND M. RAPKIN. Microdosimetry near the Trajectory of High-Energy Heavy Ions .....	183
EINAR SAGSTUEN, ELI O. HOLE, WILLIAM H. NELSON, AND DAVID M. CLOSE. ESR/ENDOR Study of Guanosine 5'-Monophosphate (Free Acid) Single Crystals X-Irradiated at 10 K .....	196
LISA R. KARAM, MIRAL DIZDAROGLU, AND MICHAEL G. SIMIC. Intramolecular H Atom Abstraction from the Sugar Moiety by Thymine Radicals in Oligo- and Polydeoxynucleotides .....	210
PHILIP J. TOFILON AND RAYMOND E. MEYN. Influence of Cellular Differentiation on Repair of Ultraviolet-Induced DNA Damage in Murine Proadipocytes .....	217
S. E. SWEIGERT, R. ROWLEY, R. L. WARTERS, AND L. A. DETHLEFSEN. Cell Cycle Effect on the Induction of DNA Double-Strand Breaks by X Rays .....	228
JAMES E. CLEAVER. Proximity of Repair Patches to Persistent Pyrimidine Dimers in DNA of Normal Human and Xeroderma Pigmentosum Cells .....	245
G. GUEDENEY, D. GRUNWALD, J. L. MALARBET, AND M. T. DOLOY. Time Dependence of Chromosomal Aberrations Induced in Human and Monkey Lymphocytes by Acute and Fractionated Exposure to <sup>60</sup> Co .....	254
E. POLIG, W. S. S. JEE, R. B. DELL, AND F. JOHNSON. Microdistribution and Local Dosimetry of <sup>226</sup> Ra in Trabecular Bone of the Beagle .....	263
M. H. SCHNEIDERMAN, K. G. HOFER, AND G. S. SCHNEIDERMAN. Cell Progression after Selective Irradiation of DNA during the Cell Cycle .....	283
H. ROOS, W.-H. THOMAS, M. FITZEK, AND A. M. KELLERER. <i>His</i> <sup>+</sup> Reversions Caused in <i>Salmonella typhimurium</i> by Different Types of Ionizing Radiation .....	292
MARY PAT FELLEZ AND LEO E. GERWECK. Influence of Extracellular pH on Intracellular pH and Cell Energy Status: Relationship to Hyperthermic Sensitivity .....	305
BARRY S. ROSENSTEIN. The Induction of DNA Strand Breaks in Normal Human Skin Fibroblasts Exposed to Solar Ultraviolet Radiation .....	313
SANG HIE KIM, SEONG SU HONG, ALAN A. ALFIERI, AND JAE HO KIM. Interaction of Hyperthermia and Pentamidine in HeLa S-3 Cells .....	320
K. KIAN ANG, HOWARD D. THAMES, SANDRA D. JONES, GUO-LIANG JIANG, LUKA MILAS, AND LESTER J. PETERS. Proliferation Kinetics of a Murine Fibrosarcoma during Fractionated Irradiation .....	327
JAE HO KIM, SANG HIE KIM, AND ALAN A. ALFIERI. Selective Killing of Glucose-Deprived Hypoxic Cells by Hyperthermia. I. Protection by Purine Ribonucleosides .....	337
EDA T. BLOOM, MITOSHI AKIYAMA, EDWARD L. KORN, YOICHIRO KUSUNOKI, AND TAKASHI MAKINODAN. Immunological Responses of Aging Japanese A-Bomb Survivors .....	343

SHORT COMMUNICATIONS

JAMES C. GARRISON AND EDWIN M. UYEKI. The Effects of $\gamma$ Radiation on Chondrogenic Development <i>in Vitro</i> .....	356
DAVID B. RUBIN, ELIZABETH A. DRAB, WILLIAM F. WARD, AND KENNETH D. BAUER. Cell Cycle Progression in Irradiated Endothelial Cells Cultured from Bovine Aorta .....	364

NUMBER 3, DECEMBER 1988

HOWARD SHIELDS, YSBRAND HAVEN, PHILLIP J. HAMRICK, JR., AND YI MA. An ESR Study of the Radicals in X-Irradiated L- $\alpha$ -Amino-n-butyric Acid HCl Containing 1.5% L-Cysteine HCl .....	373
DAVID M. CLOSE, EINAR SAGSTUEN, AND WILLIAM H. NELSON. Radical Formation in X-Irradiated Single Crystals of Guanine Hydrochloride Monohydrate. III. Secondary Radicals and Reaction Mechanisms .....	379
C. L. SANDERS, K. E. McDONALD, AND K. E. LAUHALA. Promotion of Pulmonary Carcinogenesis by Plutonium Particle Aggregation following Inhalation of <sup>239</sup> PuO <sub>2</sub> .....	393
P. BURGMAN AND A. W. T. KONINGS. Effect of Inhibitors of Poly(ADP-Ribose) Polymerase on the Heat Response of HeLa S3 Cells .....	406

R. P. JENSH AND R. L. BRENT. The Effects of Prenatal X Irradiation on the Appearance of Reflexes and Physiologic Markers in the Neonatal Rat .....	416
ANDREI LASZLO. Regulation of the Synthesis of Heat-Shock Proteins in Heat-Resistant Variants of Chinese Hamster Fibroblasts .....	427
G. P. RAAPHORST AND E. I. AZZAM. Poly(ADP-ribose) Synthetase Inhibitors Increase Radiation and Thermal Sensitivity but Do Not Affect Thermotolerance .....	442
J. RAMSAY, H. D. SUIT, F. I. PREFFER, AND R. SEDLACEK. Changes in Bromodeoxyuridine Labeling Index during Radiation Treatment of an Experimental Tumor .....	453
ROBERT E. KRISCH AND MARYANN B. FLICK. Further Studies of the Induction and Intracellular Repair of DNA Strand Breaks Using Intranuclear SV40 as a Test System .....	462
MITSURU NENOI AND TATSUAKI KANAI. Interaction Function $\gamma(x)$ for Chinese Hamster Cells Treated with Hypertonic Phosphate-Buffered Saline after Irradiation .....	472
HERMAN D. SUIT, ROBERT SEDLACEK, GEOFFREY SILVER, CHUNG-CHENG HSIEH, EDWARD R. EPP, FRANK Q. H. NGO, WILLIAM K. ROBERTS, AND LYNN VERHEY. Therapeutic Gain Factors for Fractionated Radiation Treatment of Spontaneous Murine Tumors Using Fast Neutrons, Photons Plus O <sub>2</sub> 1 or 3 ATA, or Photons Plus Misonidazole .....	482
VINCENZO COVELLI, VINCENZO DI MAJO, MARIO COPPOLA, SIMONETTA REBESSI, CATERINA BANGRAZI, AND GINO DORIA. Late Somatic Effects in Mice after Total Lymphoid Irradiation ....	503
SUSANNA C. VANANKEREN, DAVID MURRAY, AND RAYMOND E. MEYN. Induction and Rejoining of $\gamma$ -Ray-Induced DNA Single- and Double-Strand Breaks in Chinese Hamster AA8 Cells and in Two Radiosensitive Clones .....	511
LLOYD R. KELLAND, STEPHEN M. EDWARDS, AND G. GORDON STEEL. Induction and Rejoining of DNA Double-Strand Breaks in Human Cervix Carcinoma Cell Lines of Differing Radiosensitivity .....	526
SHORT COMMUNICATION	
CHARLES R. H. KENT AND GERRY H. BLEKKENHORST. <i>In Vivo</i> Radiosensitization by Diethyl-dithiocarbamate .....	539
LETTER TO THE EDITOR	
K. J. OLSEN AND J. W. HANSEN. On the Dose-Response Relationships following the Irradiation of Amino Acids .....	547
ERRATUM	
Volume 114, Number 3, June 1988: Richard C. Miller, David J. Brenner, Charles R. Geard, Kenshi Komatsu, Stephen A. Marino, and Eric J. Hall, "Oncogenic Transformation by Fractionated Doses of Neutrons," pp.589-598 .....	550
ANNOUNCEMENT .....	551
AUTHOR INDEX FOR VOLUME 116 .....	552
CUMULATIVE SUBJECT INDEX FOR VOLUMES 113-116 .....	554

## *His*<sup>+</sup> Reversions Caused in *Salmonella typhimurium* by Different Types of Ionizing Radiation

H. ROOS, W.-H. THOMAS, M. FITZEK, AND A. M. KELLERER

*Institut für Medizinische Strahlenkunde der Universität Würzburg, Versbacher Straße 5,  
D-8700 Würzburg, Federal Republic of Germany*

ROOS, H., THOMAS, W.-H., FITZEK, M., AND KELLERER, A. M. *His*<sup>+</sup> Reversions Caused in *Salmonella typhimurium* by Different Types of Ionizing Radiation. *Radiat. Res.* **116**, 292-304 (1988).

The yield of *his*<sup>+</sup> reversions in the Ames *Salmonella* tester strain TA2638 has been determined for <sup>60</sup>Co  $\gamma$  rays, 140 kV X rays, 5.4 keV characteristic X rays, 2.2 MeV protons, 3.1 MeV  $\alpha$  particles, and 18 MeV/U Fe ions. Inactivation studies were performed with the same radiations. For both mutation and inactivation, the maximum effectiveness per unit absorbed dose was obtained for the characteristic X rays, which have a dose averaged linear energy transfer (LET) of roughly 10 keV/ $\mu$ m. The ratio of the effectiveness of this radiation to  $\gamma$  rays was 2 for inactivation and about 1.4 for the *his*<sup>+</sup> reversion. For both end points the effectiveness decreases substantially at high LET, i.e., for the  $\alpha$  particles and the Fe ions. The composition of the bottom and the top agar was the one recommended by Maron and Ames [*Mutat. Res.* **113**, 173-215 (1983)] for application in chemical mutagenicity tests. The experiments with the less penetrating radiations differed from the usual protocol by utilization of a technique of plating the bacteria on the surface of the top agar. As in an earlier study [Roos *et al.*, *Radiat. Res.* **104**, 102-108 (1985)] greatly enhanced yields of mutations, relative to the spontaneous reversion rate, were obtained in these experiments by performing the irradiations 6 h after plating, which differs from the conventional procedure to irradiate the bacteria shortly after plating. © 1988 Academic Press, Inc.

### INTRODUCTION

The *Salmonella* mutagenicity test (1) is the most widely used short term test for chemical mutagens, and it is therefore desirable to examine its response to different types of ionizing radiation. Several investigations have been performed in the past. Of special importance are the studies of Isildar and Bakale, who have made a broad investigation of the effects of sparsely ionizing radiations on six of the most common tester strains (2, 3), and the work of Imray and McPhee, which includes an assessment of the influence of plasmids (4). In the earlier investigations the test appeared to be relatively insensitive to ionizing radiation. However, this apparent lack of sensitivity resulted because brief exposures were applied shortly after plating. While this was in seeming analogy to the work with chemical mutagens, it did not account for the difference between the short duration of the irradiation and the continued presence of chemical mutagens. The mutation frequencies were greatly enhanced relative to the spontaneous rates when a modified procedure was introduced (5) where the exposures were performed at a later phase during incubation (6 h after plating). With this new method a doubling dose of only 1.3 Gy of <sup>60</sup>Co  $\gamma$  rays was found for the strain



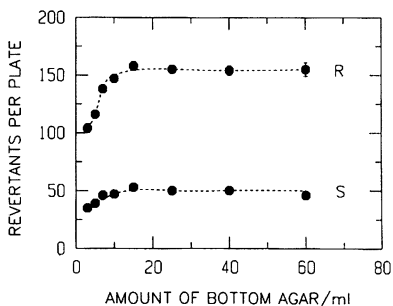


FIG. 1. Number of spontaneous revertants (S) and number of revertants (R) after exposure to 9.5 Gy of <sup>60</sup>Co  $\gamma$  rays versus the amount of bottom agar. Exposures were performed immediately after plating. A plateau at about three times higher frequency of the induced revertions was obtained for exposure with preincubation.

TA2638, and other strains showed similarly reduced doubling doses. Inactivation corrections, which were essential with the conventional method, are of less influence with the new technique.

The aim of the present study, with the improved experimental procedure, was the determination of the relative effectiveness of various ionizing radiations. There is still insufficient understanding of the different results obtained for radiation-induced mutagens in mammalian cells and in prokaryotes. In mammalian cells one finds, both for inactivation and for mutational tests such as the hypoxanthine-guanine phosphoribosyl transferase test, increased efficiencies for densely ionizing radiations with a maximum near linear energy transfer (LET) of 100 keV/ $\mu$ m (6). In their work with *E. coli* Munson and co-workers (7, 8) have found increased efficiencies of inactivation for radiations of intermediate LET. They infer from their experiments a peak at an LET of about 20 keV/ $\mu$ m, and they find a steep decrease in efficiency at higher LET. A corresponding peak was not seen in mutagenicity studies performed by these authors; they found that mutations to prototrophy of three auxotrophic strains of *E. coli* are induced with an effectiveness which decreases steadily with increasing LET. In view of these findings it seemed desirable to perform analogous studies for the *Salmonella* mutagenicity test with radiations that cover a broad range of LET. We have chosen <sup>60</sup>Co  $\gamma$  rays, 140 kV X rays (9-mm aluminum filter), 5.4 keV Cr-K $\alpha$  characteristic X rays, protons of 2.2 MeV,  $\alpha$  particles of 3.1 MeV, and, for very high LET, Fe ions of 18 MeV/U.

## MATERIALS AND METHODS

### I. Bacterial Strain

The tester strain TA2638 (*his*G428, *rfa*, pKM101) was provided by Dr. B. N. Ames, Department of Biochemistry, University of California, Berkeley.

Among a variety of tester strains, we have found particularly high mutation yields with ionizing radiations not only in TA2638 but also in TA102. The former was selected for the present studies because of its special stability and its low spontaneous reversion rate. We have also found it advantageous to use a strain which, unlike TA102, contains no plasmid carrying the *his*<sup>-</sup> site; the number of plasmids per cell is difficult to control and can be a potential source of instability in the experimental results. The genetic stability of the strain TA2638 was routinely tested for crystal-violet sensitivity (*rfa* mutation), uv sensitivity (*uvr*B

TABLE I

Half-Value Layers of the Photon Radiations and Ranges of the Charged Particles in Agar; Dose Averaged Restricted LET (100 eV Cutoff) and Dose Averaged Unrestricted LET

photons	half-value layer	$\bar{L}_{100,D}$	$\bar{L}_{\infty,D}$
$\gamma$ rays ( $^{60}\text{Co}$ )	1080 mm	5.53 keV/ $\mu\text{m}$	0.40 keV/ $\mu\text{m}$
X rays (140kV)	380 "	8.31 "	4.29 "
X rays (5.4keV)	0.23 "	11.3 "	9.66 "
charged particles	range		
Fe ions (18MeV/u)	0.480 "	469 "	1690 "
protons (2.2MeV)	0.090 "	12.3 "	15.2 "
$\alpha$ particles (3.1MeV)	0.017 "	47.9 "	132 "

mutation), and ampicillin resistance (pKM101). In a series of investigations in our laboratory, extended over about 4 years, strain TA2638 has exhibited remarkable stability in the frequency of spontaneous and radiation-induced revertants and also in inactivation yields after exposure to ionizing radiation.

## II. Preparation of Samples

The recommendations of Maron and Ames (9) have been followed with the minor modification of using a bottom-agar layer consisting of 25 ml glucose-agar medium instead of 30 ml. That this modification is of negligible influence in our experiments with ionizing radiation can be judged from the data in Fig. 1.

All chemicals were of analytical grade; water was deionized and quartz distilled. Oxoid and Difco media were used. Cultures of bacteria were started with 0.4 ml bacterial suspension from frozen permanent stocks, and plating was performed toward the end of the exponential phase (8 h). Further details have been given in the preceding publication (5).

Among the six different radiations which were employed (see Table I), two were sufficiently penetrating to permit the normal method of sample preparation in which 0.1 ml bacterial suspension (containing about  $5 \cdot 10^8$  bacteria) is mixed with 2 ml top agar and poured onto minimal glucose agar plates (diameter 85 mm). This results in a 0.3-mm top-agar layer which contains the bacteria. The number of plated bacteria is fairly uncritical in the reversion experiments with our modified technique, because the number of revertants per plate is, over a certain range, nearly independent of this parameter (5).

For the less penetrating radiations (5.4 keV characteristic X rays, 2.2 MeV protons, 3.2 MeV  $\alpha$  particles, and 18 MeV/U Fe ions) the technique of sample preparation had to be modified. This critical aspect of the experiments must be considered in some detail.

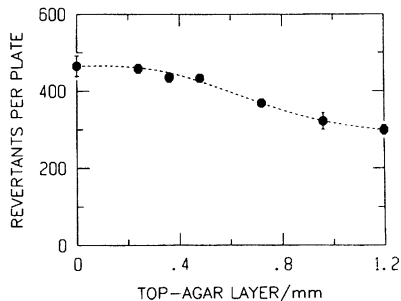


FIG. 2. Number of radiation-induced revertants per plate (revertants minus spontaneous revertants) versus thickness of the top-agar layer. The samples were exposed to 9.5 Gy of  $^{60}\text{Co}$   $\gamma$  radiation.

TABLE II

Comparison of the Surface Plating Technique and the Standard Technique

observation	number of experiments	surface-plating techn. standard technique
plating eff.	10	1.01 ± 0.01
revertants	11	1.03 ± 0.01
spont.rev.	7	1.10 ± 0.02
inactivation	20	1.03 ± 0.04

*Note.* The irradiations were performed by <sup>60</sup>Co  $\gamma$  rays. In the mutation experiments the absorbed dose was 8 Gy; different doses between 7 and 50 Gy were applied in the inactivation experiments. The errors given are standard errors.

Reduction of the amount of top agar would be one possibility to concentrate the bacteria on the surface (see Fig. 2). For zero top-agar thickness the standard supplements of 0.1  $\mu$ M D-biotin and 0.1  $\mu$ M L-histidine were mixed with the bacterial suspension, and the resulting volume of 0.3 ml was then spread directly on the bottom-agar surface. The suspension liquid enters the bottom agar, but the bacteria remain on its surface so that the radiation needs to penetrate only the bacteria (long and short diameter about 2 and 1  $\mu$ m).

In an alternative method, the 0.1 ml of bacterial suspension was spread on the surface of the solidified top agar (containing the supplement of biotin and histidine) with a Drigalski spatule. This method has been chosen for the experiments because it departs less from the standard procedure. The standard method, where the bacteria are distributed within the top-agar layer, and the surface-plating technique, where they are spread on the surface of the top agar, were compared for plating efficiency, number of spontaneous revertants, number of radiation-induced revertants, and inactivation of the bacteria by ionizing radiation (see Table II). A certain difference was seen for the frequencies of spontaneous revertants which were increased from 50 to about 55 per plate. This difference, however, is not directly relevant to the subsequent comparison of the effectiveness of different radiations which is evaluated in terms of the slope of the dose dependence.

### III. Methods of Irradiation and Dosimetry

All exposures were performed at room temperature. The dose rate of photons and  $\alpha$  particles was adjusted to 0.2 Gy/min in the mutation experiments. For technical reasons, the dose rate at the accelerators had to be higher; it was adjusted to 10 Gy/min for both the proton and the Fe ion exposures.

In the photon and  $\alpha$  particle exposures the samples were kept out of the incubator for the same time (approximately 1 h) regardless of dose. All exposures less than 10 Gy were split into two fractions with an interval chosen so that the total duration and therefore the time outside the incubator was always 50 min. The split-dose irradiations were compared with equal single doses applied either at the beginning or at the end of the 50 min period. There were no systematic differences, and one can therefore conclude that variation of the total exposure time from 10 to 50 min is of little importance.

With regard to the accelerator experiments one must still ask whether there is a time factor at the substantially higher dose rates and the short exposure times of one or a few minutes. Additional experiments were therefore performed (at the GSF, Munich) with a dose rate of 2 Gy/min <sup>60</sup>Co  $\gamma$  radiation; the results are consistent with those obtained at 0.2 Gy/min (see Fig. 3). One concludes that differences observed between photon and charged particle irradiations are not a matter of different dose rates.

In the inactivation experiments substantially higher doses were required, and this necessitated a substantially prolonged exposure time of 2 h for the highest dose, 25 Gy of  $\alpha$  rays. For the Co  $\gamma$  exposures and the soft X-ray exposures it was possible to keep the exposure times at 1 h by varying the exposure distances.

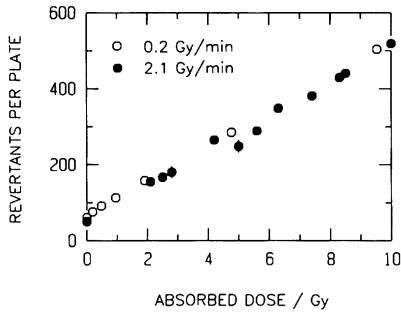


FIG. 3. Revertants per plate versus absorbed dose. The irradiations were performed with  $^{60}\text{Co}$   $\gamma$  rays, and different dose rates were compared.

Additional experiments (at the GSF, Munich) with Co  $\gamma$  rays at 25 Gy/min again did not indicate the presence of a time factor (Fig. 4). For the inactivation experiments, too, one must therefore conclude that the comparison to the accelerator experiments (10 Gy/min) is unaffected by differences in dose rate.

The  $\gamma$  exposures were performed with a  $^{60}\text{Co}$  therapy unit. Exceptions were the additional high-dose rate experiments which utilized two calibrated  $^{60}\text{Co}$  sources at the GSF, Munich.

The 140 kV X rays were produced by a 150 kV tube with beryllium window (Philips, MÖD 152 BE) operated at 140 kV and were filtered by 9 mm aluminum. Characteristic X rays were generated by a tube with Cr anode and beryllium window (Siemens, AG CR 61). The tube was operated at 10 kV to produce 5.4 keV Cr- $K\alpha$  characteristic X rays. The radiation was filtered by a 20- $\mu\text{m}$  Cr foil to reduce the bremsstrahlung (see (10)).

Photon dosimetry was performed with a calibrated therapy-dosimetry system (Dosimontor system; Dr. Pychlau GmbH, Freiburg) with suitable ionization chambers. An ionization chamber of type M 23342 was used for the dosimetry of soft X rays. A calibration factor for this chamber is usually provided for low energy photons of 8.4 keV. The calibration factor for photons of 5.4 keV is 2% in excess of the value for 8.4 keV; it was kindly provided by Dr. P. Pychlau, GmbH, Freiburg (personal communication). The chambers are calibrated for measuring exposure; conversion to absorbed dose utilized the appropriate mass-energy absorption coefficients for tissue ( $^{60}\text{Co}$   $\gamma$  rays: 37.2 Gy/(C/kg); 140 kV X rays: 34.9 Gy/(C/kg); 5.4 keV characteristic X rays: 35.7 Gy/(C/kg)). 3 MeV protons were delivered by the 3 MV van de Graaff generator of the GSF. A device to achieve homogenous irradiations of 85 mm petri dishes was constructed for this experiment (Fig. 5). The proton beam left the accelerator through a 4- $\mu\text{m}$  titanium exit foil. This foil was supported by a beam defining slit (22 mm  $\times$  0.5 mm). The sample was exposed to the beam on a

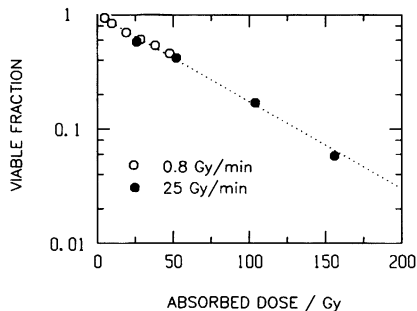


FIG. 4. Viable fraction of bacteria versus absorbed dose. The irradiations were performed with  $^{60}\text{Co}$   $\gamma$  rays, and different dose rates were compared.

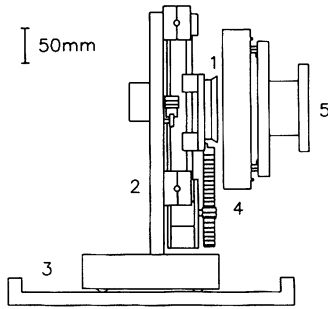


FIG. 5. Diagram of the device for proton irradiations. 1, sample; 2, scanning device (retractable from the ionization chamber for changing the sample by means of the guide way, 3); 4, ionization chamber; 5, adaptor to beam-guide tube with exit window (not visible).

computer controlled device for two-dimensional scanning. For the smallest doses a single scan was performed, for the higher doses several scans. The proton-beam current was monitored with a thin-window transmission ionization chamber located between exit window and sample. This monitor was calibrated by comparison with the proton fluence determined from etched particle tracks in Cr39 plastics. Traversal of the Ti-exit window and of the monitor ionization chamber reduced the proton energy from 3 MeV to 2.2 MeV (for details see (11)). Absorbed dose was calculated from the measured particle fluence with the LET value  $15.0 \text{ keV}/\mu\text{m}$  recommended by ICRU report 36 (12).

The construction of the  $\alpha$  irradiator is indicated in Fig. 6 (for details see (13)). Alpha particles emerging from the  $^{241}\text{Am}$  source (activity 0.37 GBq, energy of  $\alpha$  particles 5.53 MeV, diameter of active area 85 mm) are collimated to an angle less than  $12^\circ$  from the normal. The collimator removes  $\alpha$  particles which leave the source obliquely; this avoids a sharp decrease of absorbed dose with depth in the irradiated sample. To reduce energy loss, source and collimator are mounted in a container which is flushed with helium under normal pressure. In comparison to air, this reduces energy losses by a factor of more than 6. The exit foil can be thin ( $2.5 \mu\text{m}$  Mylar) since it supports no pressure differences. Petri dishes are exposed to the  $\alpha$  rays in inverted position; the distance between exit window and top agar is 1 mm. The collimator is wobbled in circular motion; this reduces the maximal difference of the fluence on the exit window from 4% for a fixed position of the collimator to less than 1%. Both values apply for a homogenous source. To improve homogeneity the source is rotated. Measured over a spot of  $6 \text{ mm}^2$  area there are maximum differences of intensity on the surface of the source of about 20%. With rotating source the corresponding maximum differences on the surface are less than 3%. The energy distribution of  $\alpha$ -particle fluence after traversal of the exit window (see Fig. 7) was measured with a semiconductor detector. The most probable  $\alpha$ -particle

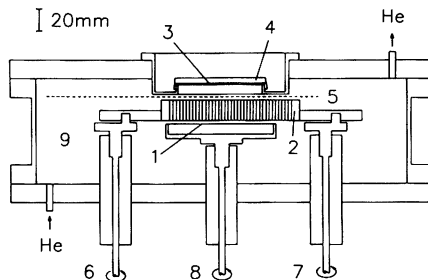


FIG. 6. Simplified view of the  $\alpha$ -irradiation device. 1, source; 2, moving collimator; 3, exit window; 4, sample; 5, shutter; 6, 7, synchronously rotating axes supporting the collimator; 8, rotating axis supporting the source-turn table; 9, helium container.

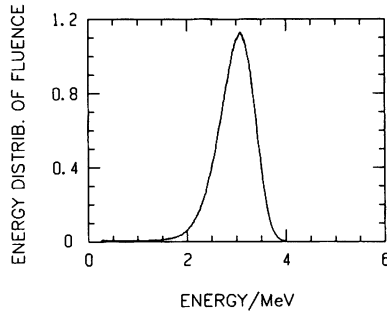


FIG. 7. Measured energy distribution of  $\alpha$ -particle fluence after traversal of the exit window.

energy is 3.1 MeV. From the data of Fig. 7 the sum distribution of remaining ranges (Fig. 8) and the depth distribution of dose in tissue (Fig. 9) was calculated with LET data from ICRU report 36.

Irradiations with 18 MeV/U Fe ions were performed at the linear accelerator UNILAC of the GSI (Darmstadt). The samples were irradiated in an exposure facility with an automatic sample changer constructed by the GSI (14). The beam was defocused and the samples were wobbled to achieve homogenous irradiations. An integrated part of the exposure facility is a secondary electron emission chamber monitoring the Fe-ion beam current. This monitor was calibrated by comparison with the particle fluence determined from track counts on etched glass samples. Absorbed dose was calculated from the measured particle fluence with LET data of Ziegler (15).

## RESULTS

The experimental results on bacterial survival and on the frequency of revertants per plate are represented in Figs. 10 and 11. In the inactivation studies the individual points are mean values for at least six plates; some points have been derived from larger numbers of plates. In most experiments data points have been obtained from repeated experiments. In the work with Fe ions at the GSI such repetitions were not possible, and all points are the result of one experiment obtained with the same bacterial culture. The data for the protons are based on two separate experiments which indicated no systematic deviations. Standard errors were derived from counts on the plates exposed to the same dose in an experiment; where they are not visible in the

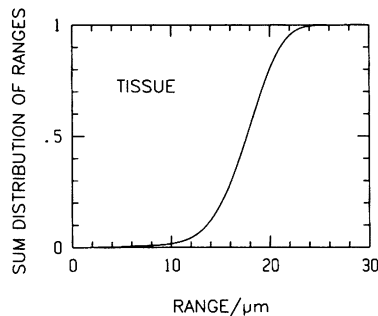


FIG. 8. Sum distribution of remaining ranges in tissue for direct exposition of the samples at the exit window.

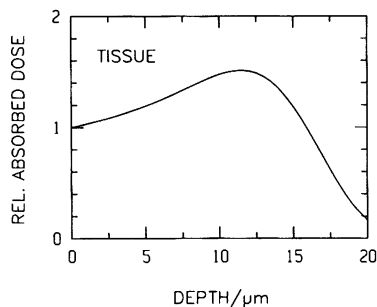


FIG. 9. Relative absorbed dose versus depth in tissue.

diagrams they are smaller than the symbols. The standard errors do not account for errors between different dose points, due for example to inaccuracies in the dilution series, nor do they account for fluctuations between experiments. The overall influ-

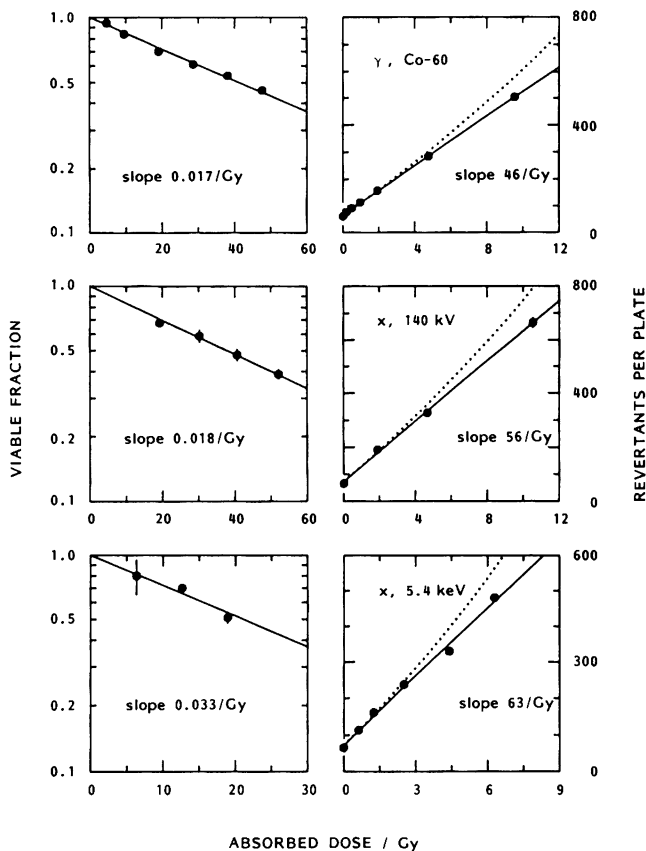


FIG. 10. Viable fraction of irradiated bacteria (left panels) and number of revertants per plate (right panels) versus absorbed dose. Samples exposed to <sup>60</sup>Co  $\gamma$  rays, 140 kV X rays filtered by 9 mm Al, and 5.4 keV Cr-K $\alpha$  characteristic X rays. Dotted lines represent the data with inactivation correction.

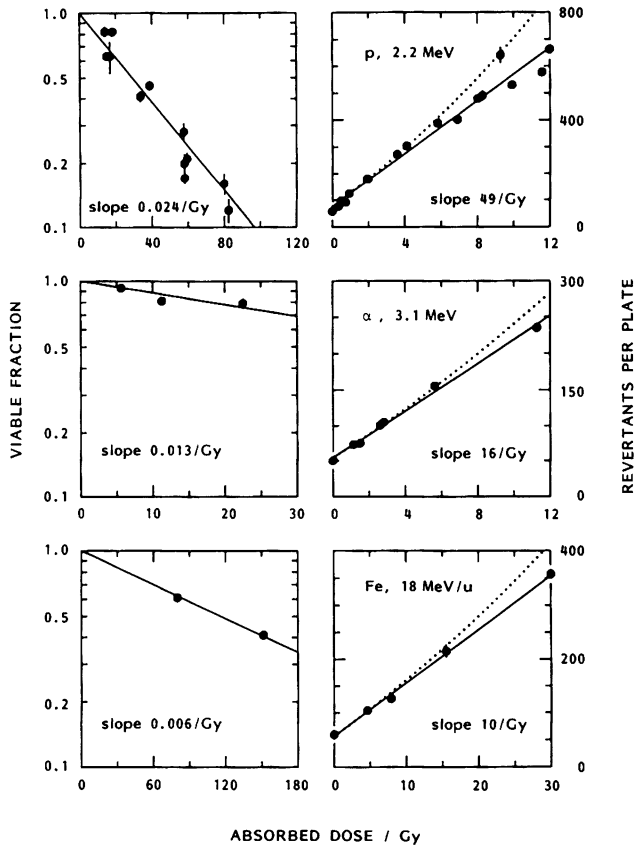


FIG. 11. Viable fraction of irradiated bacteria (left panels) and number of revertants per plate (right panels) versus absorbed dose. Samples exposed to 2.2 MeV protons, 3.1 MeV  $\alpha$  particles, and Fe ions of 18 MeV per nucleon. Dotted lines represent the data with inactivation correction.

ence of such errors can be judged from the spread of the points in individual dose-effect relations. The solid lines are least-squares fits to the observations, with equal weights for all points.

All survival curves are consistent with exponential relations. Even for the  $\gamma$  rays and the higher energy X rays there is no indication of a shoulder. With decreasing photon energy slopes are increasing. Because of the marked differences of effectiveness, different dose scales had to be used. Figure 12 serves to facilitate the comparison. The highest effectiveness for inactivation is found with 5.4 keV X rays (slope: 0.033/Gy), the lowest effectiveness with 18 MeV/U Fe ions (slope: 0.006/Gy). The numbers of revertants per plate were consistent with linear dependences on absorbed dose. Inactivation corrections were of minor influence (see dotted lines in Figs. 10 and 11), since the largest inactivated fraction corresponding to any of the points in the mutation studies was only 0.25. The mutagenicity, too, increases with decreasing photon energy; the comparison is facilitated by Fig. 13. As in the inactivation experiments,



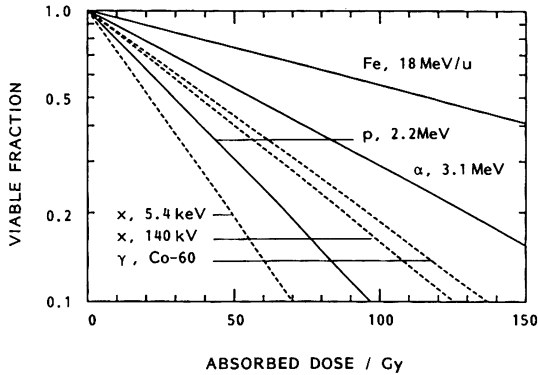


FIG. 12. Exponential functions of dose fitted to the observed viable fractions of irradiated bacteria for the six different radiations (see Figs. 10 and 11).

the soft X rays were most effective (doubling dose: 2.3 Gy), whereas the Fe ions were far less effective (doubling dose: 11.4 Gy).

#### DISCUSSION

The delayed exposure method was used for the *Salmonella* mutagenicity test to perform experiments with tester strain TA2638 (*hisG428*, *rfa*, *pKM101*) exposed to six different types of ionizing radiation. The modified method results in substantially enhanced yields of mutations, reducing the relative contribution of the spontaneous revertants and making inactivation corrections less necessary. The radiations which were employed covered a wide range of LET from sparsely ionizing  $\gamma$  rays to heavy ions of 1700 keV/ $\mu$ m. The results show a pronounced peak of inactivation for the 5.4 keV characteristic X rays. These have a dose average LET of approximately 10

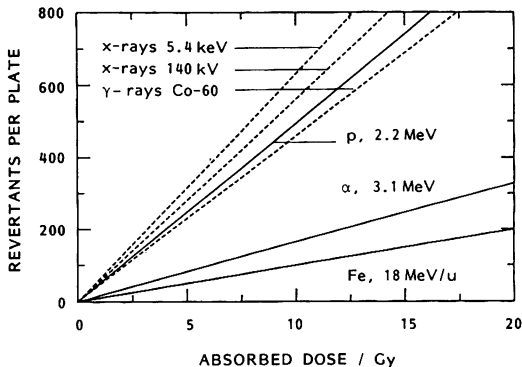


FIG. 13. Linear regressions in dose of the observed numbers of revertants per plate for the six different radiations (see Figs. 10 and 11).

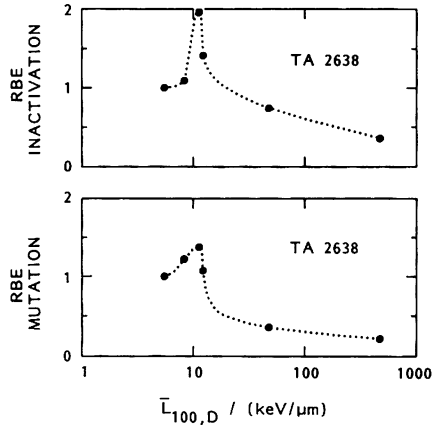


FIG. 14. RBE for inactivation (upper panel) and mutation (lower panel) of the bacteria by the different radiations. The dose average restricted LET (100 eV cutoff) is chosen as reference parameter (from left:  $^{60}\text{Co}$   $\gamma$  rays, 140 kV X rays, 5.4 keV X rays, protons,  $\alpha$  particles, Fe ions). The dotted lines are inserted for better readability of the diagrams; they have no mathematical significance.

keV/ $\mu$ m, largely independent of the cutoff that is employed. A similar but less pronounced peak is seen for the mutations.

The occurrence of a peak for inactivation at moderate values of LET is in substantial agreement with the earlier findings of Munson and colleagues (7, 8) for inactivation of *E. coli* by different types of ionizing radiation. These authors have not reported a similar peak for mutations to prototrophy in *E. coli* B/r. However, their results and the related data of Munson and Bridges (16) on bacterial phage T4 need not necessar-

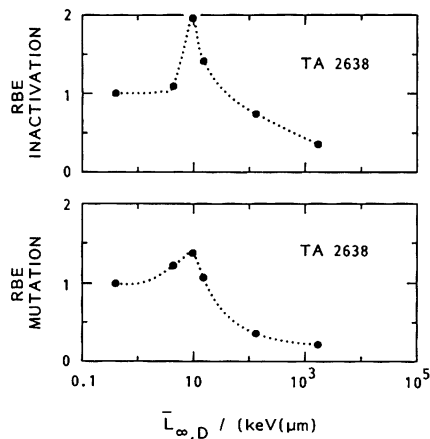


FIG. 15. RBE for inactivation (upper panel) and mutation (lower panel) of the bacteria by the different radiations. The dose average unrestricted LET is chosen as reference parameter (from left:  $^{60}\text{Co}$   $\gamma$  rays, 140 kV X rays, 5.4 keV X rays, protons,  $\alpha$  particles, Fe ions). The dotted lines are inserted for better readability of the diagrams; they have no mathematical significance.

ily be inconsistent with a peak of RBE for mutations near  $LET = 10 \text{ keV}/\mu\text{m}$ , as we see it in the present experiments. From our study one would infer that RBE values for inactivation and mutation in bacteria are largely parallel.

Various authors have developed models to link energy concentrations in cellular and subcellular structures to the effectiveness of different types of ionizing radiations in causing mutations and cell inactivation (see e.g. (17)). Such models utilize either the concept of LET or microdosimetric quantities. The microdosimetric quantities depend on the assumed target structure and size, and it would be highly tentative to relate the present observations to specific parameters. The LET concept, on the other hand, is a simplification but it has the advantage of being less closely linked to assumptions on the structure of the relevant targets. It is therefore of some interest to correlate the observed data with restricted and unrestricted LET and its mean values. Such a correlation, although largely empirical, can bring out essential features of the results.

On the basis of present radiobiological understanding it has been variously suggested that the effectiveness of different types of ionizing radiation is linked to DNA damage produced by energy concentrations on the nanometer scale. Short of a microdosimetric treatment, such energy concentrations need to be linked to restricted LET rather than total LET which includes the long-range  $\delta$  rays. Blohm and Harder (18) have held that the dose mean LET with a cutoff of 100 eV is the appropriate quantity. In the two panels of Fig. 14 the RBE for inactivation and mutation is plotted versus the dose average of restricted LET ( $\Delta = 100 \text{ eV}$ ). The averages of LET for the different radiations are based on work of Harder and Blohm (19); they are derived by averaging the contributions of the heavy particles and those of the  $\delta$  rays that exceed the cutoff energy. The inclusion of the  $\delta$  rays is essential for the protons; without this contribution they would be assigned LET values which are substantially too low. The sharp peaks in Fig. 14 are striking and may suggest that  $\bar{L}_{100,D}$  is not the suitable parameter. The soft X rays have very nearly the same mean values of restricted LET as the protons, but their effectiveness with regard to both mutation and inactivation is substantially larger. This may imply that the effect is determined not only by energy concentrations over distances of one or a few nanometers but also by energy concentrations over a larger scale. The spatial distribution of DNA and the volume of the bacterium of about  $1.6 \mu\text{m}^3$  are not inconsistent with this possibility. In view of these considerations an alternative diagram in terms of the mean values,  $\bar{L}_{\infty,D}$ , of unrestricted LET, is added in Fig. 15. With this reference parameter the peaks are still pronounced, but the comparison of the soft X rays and the protons appears less incoherent.

Possible influence of variations in dose rate has been investigated with  $\gamma$  rays. In this part of the experiment it has been found that variations in exposure time between fractions of a minute to more than an hour lead to no observed changes in inactivation probability or mutation frequency in strain TA2638. This is in line with the observed exponential relation for survival and the linear dose dependence for histidine reversions in this strain.

#### ACKNOWLEDGMENTS

This study has greatly profited from the dedicated work of Miss Renate Enßer and Miss Petra Wolf. We are especially indebted to the GSF, Munich, and to the GSI, Darmstadt for the utilization of their accelera-

tor facilities. Essential support for the irradiation experiments at the GSF has been given by Drs. F. Schulz, B. Hietel, and O. Balk. Special thanks are also due to Prof. M. Bauchinger, GSF, for technical help and permission to utilize his laboratory facilities. This work was supported by the Federal Ministry for Environment Protection and Reactor Safety of the Federal Republic of Germany—Contract St. Sch. 956. The responsibility for the results and conclusions remains with the authors.

RECEIVED: December 28, 1987; REVISED: May 17, 1988; RE-REVISED: July 11, 1988

#### REFERENCES

1. B. N. AMES, A bacterial system for detecting mutagens and carcinogens. In *Mutagenic Effects of Environmental Contaminants* (E. Sutton and M. Harris, Eds.), pp. 57–66. Academic Press, New York, 1972.
2. M. ISILDAR and G. BAKALE, Radiation-induced mutagenicity and lethality in Ames tester strains of *Salmonella*. *Radiat. Res.* **100**, 396–411 (1984).
3. M. ISILDAR and G. BAKALE, Comparative lethal effects of uv and ionizing radiation in Ames tester strains of *Salmonella*. *Radiat. Res.* **103**, 461–465 (1985).
4. F. P. IMRAY and D. G. MACPHEE, Mutagenesis by ionizing radiation in strains of *Salmonella typhimurium* used in the Ames test. *Int. J. Radiat. Biol.* **40**, 111–115 (1981).
5. H. ROOS, W. -H. THOMAS, and A. M. KELLERER, Enhanced response of the *Salmonella* mutagenicity test to ionizing radiations. *Radiat. Res.* **104**, 102–108 (1985).
6. R. COX and W. K. MASSON, Mutation and inactivation of cultured mammalian cells exposed to beams of accelerated heavy ions, III. Human diploid fibroblasts. *Int. J. Radiat. Biol.* **36**, Vo. 2, 149–160 (1979).
7. R. J. MUNSON, G. J. NEARY, B. A. BRIDGES, and R. J. PRESTON, The sensitivity of *Escherichia coli* to ionizing particles of different LETs. *Int. J. Radiat. Biol.* **13**, 205–224 (1967).
8. R. J. MUNSON and B. A. BRIDGES, Lethal and mutagenic lesions induced by ionizing radiations in *E. coli* and DNA strand breaks. *Biophysik* **6**, 1–5 (1967).
9. D. M. MARON and B. N. AMES, Revised methods for the *Salmonella* mutagenicity test. *Mutat. Res.* **113**, 173–215 (1983).
10. H. MODLER, R. BLOHM, K. -P. HERMANN, and D. HARDER, Photonenspektren, Elektronenspektren und Dosisumrechnungsfaktoren für weiche und ultraweiche Röntgenstrahlung. *Medizinische Physik 1984* (Th. Schmidt, Ed.), pp. 375–378. JSBN 3-925218-01-7.
11. H. ROOS and A. M. KELLERER, An Irradiation Device for Microbiological Studies with Charged Particle Accelerators. IMSK 87/111, 1987.
12. ICRU, *Microdosimetry*: Report 36, International Commission on Radiation Units and Measurements, Bethesda, Maryland, 1983.
13. H. ROOS and A. M. KELLERER, *An Alpha-Irradiation Device for Cell Studies*. IMSK 86/108, 1986.
14. G. KRAFT, H. W. DAUES, B. FISCHER, U. KOPF, H. P. LIEBOLD, D. QUIS, H. STELZER, J. KIEFER, R. SCHÖPFER, E. SCHNEIDER, U. WEBER, H. WULF, H. DERTINGER, Irradiation chamber and sample changer for biological samples. *Nuclear Instrum. Methods* **168**, 175–179 (1980).
15. J. F. ZIEGLER, *Handbook of Stopping Cross-Sections for Energetic Ions in All Elements*. Pergamon, New York, 1980.
16. R. J. MUNSON and B. A. BRIDGES, The LET factor in mutagenesis by ionizing radiations I. Reversion to wild type of a bacteriophage T4 amber mutant. *Int. J. Radiat. Biol.* **24**, 257–273 (1973).
17. D. T. GOODHEAD, Biophysical models of radiation action. In *Radiation Research* (E. M. Fielden, J. F. Fowler, J. H. Hendry, and D. Scott, Eds.), Taylor & Francis, London, 1987. [Abstract]
18. R. BLOHM and D. HARDER, Restricted LET: Still a good parameter of radiation quality for electrons and photons. *Radiat. Protect. Dosim.* **13**, 377–381 (1985).
19. D. HARDER and R. BLOHM, Microdosimetric characterisation of photon and electron radiations. *Radiat. Protect. Dosim.* **9**, 171–174 (1984).

## Author Index for Volume 116

- |   |   |   |
|---|---|---|
| <p style="text-align: center;"><b>A</b></p> <p>AKIYAMA, MITOSHI, 343<br/>                     ALFIERI, ALAN A., 320, 337<br/>                     ANG, K. KIAN, 327<br/>                     AUSTIN, DONALD F., 3<br/>                     AZZAM, E. I., 442</p> <p style="text-align: center;"><b>B</b></p> <p>BANGRAZI, CATERINA, 503<br/>                     BAUER, KENNETH D., 364<br/>                     BELL, C. M. JANINE, 3<br/>                     BELLI, JAMES A., 124<br/>                     BERRINO, FRANCO, 3<br/>                     BJÖRKHOLM, ELISABETH, 3<br/>                     BLEKKENHORST, GERRY H., 539<br/>                     BLETNER, MARIA, 3<br/>                     BLOOM, EDA T., 343<br/>                     BOICE, JOHN D., JR., 3<br/>                     BOSCH, ANTONIO, 3<br/>                     BRABY, L. A., 183<br/>                     BRENNER, D. J., 172<br/>                     BRENT, R. L., 416<br/>                     BURGMAN, P., 406</p> <p style="text-align: center;"><b>C</b></p> <p>CHOI, N. WON, 3<br/>                     CLEAVER, JAMES E., 245<br/>                     CLOSE, DAVID M., 196, 379<br/>                     COLEMAN, MICHEL P., 3<br/>                     COOKFAIR, DIANE L., 3<br/>                     COPPOLA, MARIO, 503<br/>                     COVELLI, VINCENZO, 503</p> <p style="text-align: center;"><b>D</b></p> <p>DEBIEU, D., 74<br/>                     DELL, R. B., 263<br/>                     DESCHAVANNE, P. J., 74<br/>                     DETHLEFSEN, L. A., 228<br/>                     DEWEY, WILLIAM C., 157<br/>                     DI MAJO, VINCENZO, 503<br/>                     DIZDAROGLU, MIRAL, 210<br/>                     DOLOY, M. T., 254</p> | <p style="text-align: center;"><b>D</b></p> <p>DORIA, GINO, 503<br/>                     DRAB, ELIZABETH A., 364</p> <p style="text-align: center;"><b>E</b></p> <p>EDWARDS, STEPHEN M., 526<br/>                     ELLETT, WILLIAM H., 173<br/>                     ENGHOLM, GÖRAN, 3<br/>                     EPP, EDWARD R., 482</p> <p style="text-align: center;"><b>F</b></p> <p>FELLEENZ, MARY PAT, 305<br/>                     FERTIL, B., 74<br/>                     FITZEK, M., 292<br/>                     FLICK, MARYANN B., 462<br/>                     FOWLER, J. F., 175<br/>                     FRASER, PATRICIA, 3<br/>                     FRIEDMAN, LIBBY R., 89<br/>                     FRISCHKORN, ROLF, 3<br/>                     FRY, R. J. M., 1</p> <p style="text-align: center;"><b>G</b></p> <p>GARRISON, JAMES C., 356<br/>                     GERWECK, LEO E., 305<br/>                     GORODETSKY, RAPHAEL, 135<br/>                     GRIEM, M. L., 176<br/>                     GRUNWALD, D., 254<br/>                     GUEDENEY, G., 254<br/>                     GUPTA, VICRAM, 124</p> <p style="text-align: center;"><b>H</b></p> <p>HAMRICK, PHILLIP J., JR., 373<br/>                     HANSEN, J. W., 547<br/>                     HANSON, WAYNE R., 145<br/>                     HAVEN, YSBRAND, 373<br/>                     HERRLICH, PETER, 178<br/>                     HISLOP, T. GREGORY, 3<br/>                     HOFER, K. G., 283<br/>                     HOLE, ELI O., 196<br/>                     HONG, SEONG SU, 320<br/>                     HOWARD, J., 183<br/>                     HSIEH, CHUNG-CHENG, 482<br/>                     HUTCHISON, GEORGE B., 3</p> | <p style="text-align: center;"><b>J</b></p> <p>JEE, W. S. S., 263<br/>                     JENSH, R. P., 416<br/>                     JIANG, GUO-LIANG, 327<br/>                     JOHNSON, F., 263<br/>                     JONES, SANDRA D., 327</p> <p style="text-align: center;"><b>K</b></p> <p>KAMPINGA, HARM H., 114<br/>                     KANAI, TATSUAKI, 472<br/>                     KARAM, LISA R., 210<br/>                     KELLAND, LLOYD R., 526<br/>                     KELLERER, A. M., 292<br/>                     KENT, CHARLES R. H., 539<br/>                     KEYES, SUSAN R., 100<br/>                     KIM, JAE HO, 320, 337<br/>                     KIM, SANG HIE, 320, 337<br/>                     KIRN, VERA POMPE, 3<br/>                     KJØRSTAD, KJELL E., 3<br/>                     KLEINERMAN, RUTH A., 3<br/>                     KLIAUGA, P. J., 183<br/>                     KOCH, MARIA, 3<br/>                     KONDO, TAKASHI, 56<br/>                     KONINGS, A. W. T., 406<br/>                     KONINGS, ANTONIUS W. T., 114<br/>                     KORN, EDWARD L., 343<br/>                     KREIGER, NANCY, 3<br/>                     KREMENTZ, EDWARD T., 3<br/>                     KRISCH, ROBERT E., 462<br/>                     KRISHNA, C. MURALI, 56<br/>                     KUSUNOKI, YOICHIRO, 343</p> <p style="text-align: center;"><b>L</b></p> <p>LASZLO, ANDREI, 427<br/>                     LATOURETTE, HOWARD B., 3<br/>                     LAUHALA, K. E., 393<br/>                     LISCO, HERMANN, 3<br/>                     LOCHMÜLLER, H., 3</p> <p style="text-align: center;"><b>M</b></p> <p>MA, YI, 373<br/>                     MACMAHON, BRIAN, 3</p> |
|---|---|---|

MAKINODAN, TAKASHI, 343  
 MALAISE, E. P., 74  
 MALARBET, J. L., 254  
 MALKINSON, FREDERICK D., 145  
 MCBRIDE, WILLIAM H., 135  
 McDONALD, K. E., 393  
 MERRILL, JAMES A., 3  
 METTING, N. F., 183  
 MEYN, RAYMOND E., 217, 511  
 MILAS, LUKA, 327  
 MOLONEY, WILLIAM C., 3  
 MURRAY, DAVID, 511

## N

NEAL, FRANK E., 3  
 NELSON, WILLIAM H., 196, 379  
 NENOI, MITSURU, 472  
 NGO, FRANK Q. H., 482

## O

OLEINICK, NANCY L., 89  
 OLSEN, K. J., 547

## P

PANIZZON, RENATO G., 145  
 PEJOVIC, MARIE-HÉLÈNE, 3  
 PETERS, LESTER J., 3, 327  
 PETERSSON, FOLKE, 3  
 POLIG, E., 263  
 PREFFER, F. I., 453  
 PRIOR, PATRICIA, 3

## R

RAAPHORST, G. P., 442  
 RAMSAY, J., 453  
 RAPKIN, M., 183  
 REBESSI, SIMONETTA, 503  
 RIESZ, PETER, 56  
 RIMPELA, ARJA, 3  
 ROBB, DOROTHY, 3  
 ROBERTS, WILLIAM K., 482  
 ROBSON, DIANE, 3  
 ROCKWELL, SARA, 100  
 ROOS, H., 292  
 ROSENSTEIN, BARRY S., 313  
 ROSSI, H. H., 183  
 ROTI ROTI, JOSEPH L., 114  
 ROWLEY, R., 228  
 RUBIN, DAVID B., 364

## S

SAGSTUEN, EINAR, 196, 379  
 SANDERS, C. L., 393  
 SARTORELLI, ALAN C., 100  
 SCHIMMERLING, W., 183  
 SCHNEIDERMAN, G. S., 283  
 SCHNEIDERMAN, M. H., 283  
 SCHULZ, MILFORD D., 3  
 SCHWARTZ, DAVID E., 145  
 SEDLACEK, R., 453  
 SEDLACEK, ROBERT, 482  
 SHIELDS, HOWARD, 373  
 SIGURDSSON, KRISTJAN, 3  
 SILVER, GEOFFREY, 482  
 SIMIC, MICHAEL G., 210  
 STANKUSOVA, HANNA, 3  
 STEEL, G. GORDON, 526

STORM, HANS H., 3  
 STOVALL, MARILYN, 3  
 SUIT, H. D., 453  
 SUIT, HERMAN D., 482  
 SWEIGERT, S. E., 228

## T

THAMES, HOWARD D., 327  
 THOMAS, W.-H., 292  
 THOMSON, D. H., 3  
 TOFILON, PHILIP J., 217

## U

UYEKI, EDWIN M., 356

## V

VANANKEREN, SUSANNA C., 511  
 VERHEY, LYNN, 482  
 VIDAIR, CHARLES A., 157  
 VON FOURNIER, DIETRICH, 3

## W

WARD, WILLIAM F., 364  
 WARTERS, R. L., 228  
 WITHERS, H. RODNEY, 135  
 WONG, M., 183  
 WRIGHT, WILLIAM D., 114

## X

XUE, LIANG-YAN, 89

## Z

ZAIDER, M., 183

## Cumulative Subject Index<sup>1</sup>

### Volumes 113–116

#### A

##### Acknowledgment

manuscript reviewers, **114**, 641

##### Adenine

formation in  $\gamma$ -irradiated adenosine 5'-monophosphate solutions, role of oxygen, **113**, 447

##### Adenosine 5'-monophosphate

$\gamma$  irradiation, oxygen dependence of product formation, **113**, 447

##### Adipose tissue

normal, response to graduated doses of hyperthermia (pig), **114**, 225

##### Amino acids

irradiation, dose-response relationships, letter to the editor, **111**, 374; reply, **116**, 547

##### 3-Aminobenzamide

effect on

cell survival after X irradiation (CHO HA-1 cells), **114**, 186

heat sensitivity of HeLa cells, **116**, 406

thermotolerance and heat and radiation responses (V79 cells), **116**, 442

##### 4-Aminobenzamide

effect on heat sensitivity of HeLa cells, **116**, 406

##### L- $\alpha$ -Amino-*n*-butyric acid hydrochloride

system containing 1.5% L-cysteine HCl, X irradiation, ESR study of generated radicals, **116**, 373

##### 2-[(Aminopropyl)amino]ethanethiol, *see* WR-1065

##### S-2-(3-Aminopropylamino)ethylphosphorothioic acid, *see* WR-2721

##### Anesthesia

pentobarbital, effects on tumor energy metabolism *in vivo*, analysis by <sup>31</sup>P NMR spectroscopy (mouse), **115**, 361

##### Angiogenesis

capillary, *in vivo* inhibition by hyperthermia, analysis (mouse), **114**, 297

#### Announcements

American Endocurietherapy Society, 11th Annual Mid-Winter Meeting, Marco Island, Florida, December 1988, **115**, 212

American Radium Society, 71st Annual Meeting, St. Thomas, U.S. Virgin Islands, April 1989, **115**, 387

American Society for Photobiology, 10th International Congress, Jerusalem, Israel, October–November 1988, **114**, 399

Course on Pathologic Effects of Radiation, Bethesda, Maryland, June 1988, **113**, 204

European Society for Radiation Biology, 21st Annual Scientific Meeting, Tel Aviv, Israel, October 1988, **114**, 200, 399

European Society for Therapeutic Radiology and Oncology, Seventh Annual Meeting, The Hague, The Netherlands, September 1988, **114**, 399

Health Physics Society, Midyear Topical Meeting, San Antonio, Texas, December 1988, **114**, 399

Health Physics Society, Thirty-third Annual Meeting, Boston, Massachusetts, July 1988, **114**, 399

Indian Association of Chemotherapists, Fifth Biennial Conference, Bombay, India, February 1989, **115**, 630

International Conference: Ionizing Radiation and Cancer Epidemiology, Edgbaston, Birmingham, England, July 1989, **116**, 551

National Council on Radiation Protection and Measurements, Twenty-fifth Annual Meeting, Washington, D.C., April 1989, **116**, 181

Radiation Research Society 37th Annual Meeting and North American Hyperthermia Group 9th Annual Meeting, Seattle, Washington, March 1989, **115**, 211

Society for Risk Analysis, Fifth Annual Meeting, Washington DC, October–November 1988, **114**, 399

<sup>1</sup> Boldface numbers indicate appropriate volume; lightface numbers indicate pagination.

- Workshop on Biomedical Uses of Heavy Ions at BEVALAC, Berkeley, California, March 1989, **115**, 630
- Anserine  
radioprotection of bacteriophages T4 and P22 against  $\gamma$  irradiation inactivation, **114**, 319
- Antibiotics  
in management of postirradiation local and systemic infections, review, **115**, 1
- Antigens  
tumor-specific, radiation-induced expression, analysis in cell hybrids (human), **114**, 84
- $\beta$ -Arabinofuranosyladenine  
effect on X-ray-induced chromosome damage in plateau-phase CHO cells: implications for repair and fixation of  $\alpha$ -potentially lethal damage, **114**, 361
- 1- $\beta$ -D-Arabinofuranosylcytosine  
detectable sites in DNA, induction by X and  $\gamma$  irradiation, comparison (human), **114**, 168
- Arabinose  
hypertonic, modified blood-brain barrier, uptake of WR-2721 into brain (rat), **115**, 303
- Argon ions  
accelerated, effect on retina (rat), **115**, 192  
and X rays, sequential exposure of fibroblasts: damage interaction effects as function of cell cycle stage (V79 cells), **115**, 54
- Atomic bomb  
Hiroshima and Nagasaki,  $\gamma$  doses, reassessment, **113**, 1  
Hiroshima, thermoluminescence dosimetry measurements of  $\gamma$  radiation by predose technique, **113**, 227
- Atomic bomb survivors  
cancer mortality risk estimates, effect of changes in dosimetry, **114**, 437  
in Hiroshima, immune responses, assessment, **116**, 343
- Attenuation coefficients  
photon, and dose-spread kernels, relationships, **113**, 235
- B**
- Bacteria  
*Escherichia coli*  
radioprotection by cysteamine, mechanisms, **114**, 550  
*thyA* mutants,  $\gamma$ -irradiated, effects of dihydrothymine and thymine glycol on pyrimidine salvage and thymineless radiosensitization, **115**, 617  
and wild-type eukaryotes, uv action spectra (254–320 nm), comparison, **114**, 307  
interactive killing effects between X rays and uv rays or nitrogen mustard, quantitative aspects, **115**, 124  
*Salmonella typhimurium*, *his*<sup>+</sup> reversions induced by various types of ionizing radiation, comparative analysis, **116**, 292
- Bacteriophages  
T4 and P22, inactivation by  $\gamma$  irradiation, radioprotective effects of ergothioneine, histidine, carnosine, and anserine, **114**, 319
- BEIR IV Report  
calculational error in risk estimates for lung cancer due to radon, letter to editor, **116**, 173
- Benzamide  
effect on thermotolerance and heat and radiation responses (V79 cells), **116**, 442
- Beta irradiation  
skin, 100% tumor induction after repeated doses in limited range (mouse), **115**, 488
- 1,3-Bis(2-chloroethyl)-1-nitrosourea  
and X rays, additive induction of sister chromatid exchange in brain tumor cells (rat), **115**, 187
- Blood-brain barrier  
hypertonic arabinose-modified, uptake of WR-2721 into brain (rat), **115**, 303
- Blood flow  
cerebral  
changes after  $\gamma$  irradiation, analysis in glioma model (rat), **115**, 586  
local, effect of ionizing radiation-induced emesis (ferret), **114**, 537  
tumor  
effects of inhalational or injectable anesthetics and of neuroleptic, neuroleptanalgesic, and sedative agents (rat), **114**, 64  
hydralazine-induced reduction after X irradiation, effect on efficacy of misonidazole and RSU-1069 (mouse), **115**, 292  
RIF-1, effect of treatment with etomidate and Gibbs clip (mouse), **114**, 105
- Body temperature  
irradiation-induced responses, role of prostaglandins and histamine H<sub>1</sub> and H<sub>2</sub> receptors (rat), **114**, 42
- Bone  
trabecular, microdistribution and local dosimetry of <sup>226</sup>Ra after iv injection (dog), **116**, 263
- Bone marrow  
 $\gamma$ -irradiated, recovery of hemopoietic and stromal progenitor cells, effect of low dose rate (mouse), **115**, 481  
tetrachlorodecaoxide effects after whole-body  $\gamma$  irradiation (rat), **115**, 115



- transplantation, role in treatment of nuclear accident victims, **113**, 205
- Book reviews  
 Innovations in Radiation Oncology, H. R. Withers and L. J. Peters (Eds.), 1988, **116**, 176  
 Radiobiology for the Radiologist, 3rd ed., E. J. Hall, 1988, **116**, 175
- Brain  
 area postrema, chronic lesions, effect of radioemetic protection at 24 hours (cat), **114**, 77  
 $\gamma$  irradiation, associated blood flow changes, analysis in glioma model (rat), **115**, 586  
 heavy ion irradiation, subsequent NMR imaging and spectroscopy (rat), **113**, 79  
 local blood flow, effect of ionizing radiation-induced emesis (ferret), **114**, 537  
 WR-2721 entry across modified blood-brain barrier (rat), **115**, 303  
 X irradiation, alterations of neuronal chromatin structure (rat), **114**, 94
- Bromodeoxyuridine  
 pulse-labeled fibrosarcoma cells, changes in labeling index during radiation treatment (mouse), **116**, 453
- t*-Butanol  
 influence on sulfhydryl protection and oxygen effect on radiation-induced inactivation of r-chromatin *in vitro* (*Tetrahymena*), **115**, 141  
 protective effects on radiation-induced inactivation of isolated transcriptionally active chromatin: influence of secondary radicals (*Tetrahymena*), **114**, 28
- L-Buthionine sulfoximine  
 and dimethylfumarate, acute depletion of glutathione, toxic effects on mammary carcinoma cells (mouse), **114**, 215
- C**
- Caffeine  
 modulation of X-ray lethal action on fibroblasts (V79 cells), **115**, 176
- Calcium  
 dependent cellular processes, induction by hyperthermia, role in thermoresistance (Chinese hamster lung, Morris hepatoma cells), **113**, 426  
 intracellular levels  
 in cells and tissues, relationship to heat shock-induced protein synthesis and cytoskeletal rearrangements (*Drosophila melanogaster*), **113**, 402  
 effect of hyperthermia (mammalian cells), **113**, 414  
 role in heat-induced cell injury, symposium introduction, **113**, 401
- Calorimetry  
 measurements of carbon kerma factor for 14.6-MeV neutrons, correction, **113**, 396; reply, **113**, 398
- Cancer  
 cervical, patients receiving radiotherapy: relationship between dosage and second cancer risk, **116**, 3  
 mortality risk estimates in atomic bomb survivors, effect of changes in dosimetry, **114**, 437  
 relative risk, for radiogenic neoplasms, extrapolation across mouse strains and to man, **114**, 331  
 therapy, potential applicability of nonclonogenic measurements (human), **114**, 401
- Carcinogenesis  
 pulmonary, promotion by plutonium particle aggregation after  $^{239}\text{PuO}_2$  inhalation (rat), **116**, 393  
 radiotherapy-induced, in patients with cervical cancer: relationship between radiation dose and cancer risk, **116**, 3  
 X-ray-induced, effect of hyperthermia (mouse), **115**, 448
- Cardiomyopathy  
 radiation-induced, analysis (dog), **113**, 120
- Cardiovascular function  
 effect of chronic  $^{239}\text{PuO}_2$  inhalation exposure (dog), **115**, 314
- Carnosine  
 radioprotection of bacteriophages T4 and P22 against  $\gamma$  irradiation inactivation, **114**, 319
- Catalase  
 increased activity in stable  $\text{H}_2\text{O}_2$ -resistant variants of CHO HA-1 cells, analysis, **114**, 114
- Cataracts  
 incidence in patients injected with  $^{224}\text{Ra}$ , epidemiological analysis, **115**, 238
- Cell cultures  
 cerebral gliosarcoma cells in monolayers and spheroids, repair of potentially lethal damage and reentry into cycling phase after X irradiation, comparison (rat), **114**, 515  
 limb bud, chondrogenic development, effects of  $\gamma$  radiation (chicken embryo), **116**, 356
- Cell cycle  
 effect on X-ray-induced DNA double- and single-strand breaks, comparison (murine mammary tumor cells), **116**, 228  
 $\text{G}_2$  arrest in X-irradiated CHO cells, effects of poly(adenosinediphosphoribose) synthesis inhibitors and structurally related compounds, **113**, 58  
 $\gamma$ -ray-sensitive XR-1 cells, role in repair of potentially lethal damage, **115**, 325

- progression in aortic endothelial cells after  $\gamma$  irradiation, analysis (bovine), **116**, 364
- quiescence, stimulation of lens epithelial cells from, subsequent sensitivity to X-ray-induced growth arrest (rat), **113**, 133
- selective  $^{125}\text{I}$  irradiation of DNA during, effects on cell progression (CHO cells), **116**, 283
- S phase, delay in initiation of DNA synthesis after irradiation, effect of oxygen (murine melanoma), **113**, 102
- stage-dependent influence on damage interaction effects after sequential exposures to high- and low-LET radiations (V79 cells), **115**, 54
- synchronized neuroblastoma cells, proliferation after heat treatment, role of heat-shock proteins (mouse), **113**, 252
- synchronous G1 and S phase CHO cells, hyperthermic cell killing *in vitro*, time-temperature analyses, **113**, 318
- X-irradiated cerebral gliosarcoma cells grown as monolayers and spheroids, comparative analysis (rat), **114**, 515
- Cell killing
- hyperthermic
    - CHO cells in plateau phase, analysis of rapid and slow modes, **116**, 157
    - effect of pentamidine (HeLa cells), **116**, 320
    - hypoxic glucose-deprived HeLa cells, protection by purine ribonucleosides, **116**, 337
    - and mitogenic response to serum and growth factors, relationship (CHO HA-1 cells), **113**, 501
    - role of
      - $\text{Ca}^{2+}$ , symposium introduction, **113**, 401
      - poly(ADP-ribose)polymerase (HeLa cells), **116**, 406
    - and serum starvation, effect on viability of CHO HA-1 cells, **113**, 513
    - synchronous G1 and S phase CHO cells *in vitro*, time-temperature analyses, **113**, 318
    - induced by *N*-methyl-*N'*-nitro-*N*-nitrosoguanidine, effect of  $\gamma$  preirradiation (V79 cells), **115**, 609
    - leukemia cells by very low dose rate  $\gamma$  irradiation (mouse), **115**, 273
    - RIF-1 tumor cells with 8-hydroxyquinoline, evaluation (mouse), **115**, 373
- Cell lines, *see also* Tumor cells
- 023 (Chinese hamster lung), thermoresistance, role of hyperthermia-induced  $\text{Ca}^{2+}$ -dependent cellular responses, **113**, 426
  - AA3 (Chinese hamster ovary), and radiosensitive clones
    - DNA strand breaks, induction and rejoining after  $\gamma$  irradiation, **116**, 511
    - survival and recovery after  $\gamma$  irradiation, **115**, 223
  - A<sub>L</sub> (human  $\times$  hamster hybrid), neutron irradiation, mutation induction and relative biological effectiveness, **115**, 281
  - CC91 (human fibroblasts), infection with  $\gamma$ -irradiated simian virus 40: intracellular induction and repair of viral DNA strand breaks, analysis, **116**, 462
  - CGL1 (HeLa  $\times$  skin fibroblasts), radiation-induced expression of tumor-specific antigen, analysis, **114**, 84
  - CHO (Chinese hamster ovary), *see* CHO cells
  - CV-1 (African green monkey kidney), infection with  $\gamma$ -irradiated simian virus 40: intracellular induction and repair of viral DNA strand breaks, analysis, **116**, 462
  - HeLa (human cervical carcinoma), *see* HeLa cells
  - Kc (*Drosophila melanogaster*), intracellular free  $\text{Ca}^{2+}$  levels, relationship to heat shock-induced protein synthesis and cytoskeletal rearrangements, **113**, 402
  - L5178Y-R and L5178Y-S (murine lymphoblastic leukemia), radiosensitivity and repair of potentially lethal and sublethal damage, effects of reduced temperature and starvation conditions, **113**, 458
  - TN-368 (*Trichoplusia ni*)
    - $\gamma$ -irradiated, recovery enhancement by split-dose treatment, **115**, 413
    - radiosensitivity and DNA double-strand break repair, comparison, **113**, 268
  - V79 (Chinese hamster lung fibroblasts), *see* V79 cells
  - XR-1 (Chinese hamster ovary),  $\gamma$ -ray-sensitive, cell cycle-dependent repair of potentially lethal damage, **115**, 325
- Cervix
- cancer patients, risk of radiotherapy-induced carcinogenesis and radiation dose, relationship, **116**, 3
- Chemosensitivity
- tumor cells, assessment techniques, implications for clinical oncology (human), **114**, 401
- Chimeras
- embryo aggregation, assay for X-ray-induced nonlethal changes in preimplantation embryos (mouse), **113**, 289
- Chloral hydrate
- effect on tumor blood flow (rat), **114**, 64
- CHO cells
- DNA, selective  $^{125}\text{I}$  irradiation during cell cycle, effects on cell progression, **116**, 283

- DNA synthesis, heat effects, assessment of subsequent recovery, **114**, 125
- G<sub>2</sub> arrest induced by X irradiation, effects of poly(adenosinediphosphoribose) synthesis inhibitors and structurally related compounds, **113**, 58
- γ-ray-induced DNA single-strand breaks, radioprotective effects of WR-1065, **113**, 155
- HA-1
- heat-resistant variants, heat-shock protein synthesis regulation, analysis, **116**, 427
  - hyperthermic cell killing and serum starvation, effect on viability, **113**, 513
  - subsequent mitogenic response to serum and growth factors, **113**, 501
  - stable H<sub>2</sub>O<sub>2</sub>-resistant variants, increase in catalase activity, **114**, 114
  - survival after X irradiation, effects of sodium butyrate and 3-aminobenzamide, **114**, 186
  - viability during serum starvation and hyperthermia, **113**, 513
- heating at 45°C at pH 6.6
- development of thermotolerance and changes in intracellular pH, **115**, 106
  - relationship between intra- and extracellular pH, **115**, 96
- heat-sensitive thermotolerant defective mutants, isolation and characterization, **113**, 526
- hyperthermia-induced death in plateau phase, analysis of rapid and slow modes, **116**, 157
- hyperthermic radiosensitization, acid-induced increase, role of intracellular and extracellular pH, **115**, 576
- intracellular pH and cell energy status, effect of extracellular pH: relationship to hyperthermic sensitivity, **116**, 305
- microinjection with glutathione disulfide, induction of thermotolerance, **115**, 202
- mitochondrial damage after hyperthermic exposures, electron microscopic analysis, **115**, 421
- mitochondrial glutathione depletion, relationship to thermal sensitivity, **115**, 461
- oxygen uptake, inhibition by lonidamine, **113**, 356
- plateau-phase, X-ray-induced chromosome damage, effect of arabinofuranosyladenine, implications for repair and fixation of α-potentially lethal damage, **114**, 361
- protein synthetic mutant and wild-type cells, X irradiation: analysis of split-dose recovery and protein synthesis, **114**, 281
- radiosensitivity, effect of dimethylfumarate, **115**, 495
- sensitization to hyperthermia, role of low intracellular pH, **114**, 154
- synchronous G1 and S phase, hyperthermic cell killing *in vitro*, time-temperature analyses, **113**, 318
- Chondrogenesis
- limb bud cells *in vitro*, effects of γ radiation (chicken embryo), **116**, 356
- Chromatids
- sister, exchange in brain tumor cells, additive induction by X rays and 1,3-bis(2-chloroethyl)-1-nitrosourea (rat), **115**, 187
- Chromatin
- cerebellar neuronal, postirradiation structural alterations, analysis (rat), **114**, 94
  - damage in γ-irradiated V79 cells, repair, effects of glutathione depletion and hypoxia, **116**, 89
  - isolated transcriptionally active, radiation-induced inactivation, protection by OH scavengers: influence of secondary radicals (*Tetrahymena*), **114**, 28
  - radiation-induced inactivation *in vitro*, sulfhydryl protection and oxygen effect, influence of *t*-butanol (*Tetrahymena*), **115**, 141
  - thymic, conformational changes after microwave exposure (rabbit), **115**, 44
- Chromosomes
- damage by γ irradiation, comparison between human and murine peripheral blood lymphocytes, **115**, 334
  - and DNA
    - initial damage after X irradiation, role in radiosensitivity difference between L5178Y-R and L5178Y-S cells (mouse), **115**, 550
    - repair after X irradiation, role in radiosensitivity difference between L5178Y-R and L5178Y-S cells (mouse), **115**, 566
  - γ-ray- and fission-spectrum neutron-induced damage, radioprotective effects of WR-1065 (V79 cells), **113**, 145
  - lymphocyte, structural aberrations induced by acute and fractionated γ irradiation, time dependence (human, monkey), **116**, 254
  - in peripheral lymphocytes of Hodgkin's disease patient, structural aberrations induced by radiotherapy, **114**, 528
  - transposon- and X-ray-induced translocations and transmission distortion, interaction (*Drosophila melanogaster*), **115**, 503
  - X-ray-induced damage
    - long-term repair *in vivo* (murine hepatocytes), **113**, 40
    - in plateau-phase CHO cells, effects of arabinofuranosyladenine: implications for repair

- and fixation of  $\alpha$ -potentially lethal damage, **114, 361**
- Cisplatin**  
oxygen- and temperature-dependent cytotoxic and radiosensitizing effects on cervical carcinoma cells *in vitro* (human), **114, 489**
- Clonogens**  
hepatocyte, sensitivity to X-ray dose fractionation (mouse), **113, 51**
- Coions**  
depletion near DNA: evidence from DNA interaction with glutathione and other low-molecular-weight thiols, **114, 3**
- Collagen**  
biosynthesis in skin and skin fibroblast cultures,  $\gamma$ -ray-induced increases, 48-week study (mouse), **116, 145**  
isotypes I, III, and IV in lung, changes induced by X irradiation, effects of time, dose, and WR-2721 (mouse), **115, 515**
- Colony-forming ability**  
hepatocytes after X irradiation, long-term repair *in vivo* (mouse), **113, 40**
- Computer simulation**  
Monte Carlo method, track structures for 0.3–20-MeV protons, microdosimetric aspects, **115, 389**
- Copper**  
serum levels, evaluation as index of lung injury after hemithorax exposure to  $\gamma$  rays (rat), **114, 613**
- Cordycepin**  
and 2-halo derivatives, metabolic effects on repair of X-ray-induced potentially lethal damage in V79 cells, **114, 231**
- Counterions**  
condensation near DNA: evidence from DNA interaction with glutathione and other low-molecular-weight thiols, **114, 3**
- 8,5'-Cycloadenosine 5'-monophosphate**  
formation in  $\gamma$ -irradiated adenosine 5'-monophosphate solutions, role of oxygen, **113, 447**
- Cysteamine**  
radioprotection of *Escherichia coli*, mechanisms, **114, 550**
- Cytoskeleton**  
rearrangements, heat shock-induced, in cells and tissues, relationship to intracellular free  $\text{Ca}^{2+}$  levels (*Drosophila melanogaster*), **113, 402**
- Cytotoxicity**  
*cis*-dichlorodiammineplatinum(II) against cervical carcinoma cells *in vitro*, analysis (human), **114, 489**
- D**
- Damage**  
chromosomes,  $\gamma$ -ray- and fission-spectrum neutron-induced, radioprotective effects of WR-1065 (V79 cells), **113, 145**
- DNA**  
induction and repair in  $\gamma$ -irradiated lymphoblasts, effects of oxygen and misonidazole (human), **115, 436**  
in irradiated epithelial teratocarcinoma cells, comparison with V79 cells (human), **113, 278**  
potentially lethal, *see* Potentially lethal damage  
sublethal, *see* Sublethal damage  
3'-Deoxyadenosine, *see* Cordycepin
- Deoxyribose**  
moiety in oligo- and polydeoxynucleotides, H atom abstraction by thymine radicals, analysis, **116, 210**
- Development**  
reflex acquisition and physiologic marker appearance, effects of prenatal X irradiation (rat), **116, 416**
- Diazepam**  
effect on tumor blood flow (rat), **114, 64**
- cis*-Dichlorodiammineplatin, *see* Cisplatin
- Diethyldithiocarbamate**  
radiosensitization of tumors *in vivo* (mouse), **116, 539**
- Differentiation**  
cellular, effect on repair of DNA damage in  $\gamma$ -irradiated proadipocytes (mouse), **116, 217**
- $\alpha$ -Difluoromethylornithine  
induced polyamine depletion, effects on radiosensitivity of colon carcinoma cells (human), **114, 634**
- Dihydrothymine**  
effect on pyrimidine salvage and thymineless radiosensitization in *Escherichia coli thya* cells, **115, 617**
- Dimethylfumarate**  
and L-buthionine sulfoximine, acute depletion of glutathione, toxic effects on mammary carcinoma cells (mouse), **114, 215**  
effect on CHO cell sensitivity to X irradiation, **115, 495**
- 16,16-Dimethylprostaglandin E<sub>2</sub>**  
and/or WR-2721, radioprotection against fission neutron- $\gamma$  irradiation (mouse), **115, 605**
- Disease**  
incidence in C57Bl mouse after single and fractionated  $\gamma$  and neutron irradiations, **113, 300**

## DNA

## and chromosomes

initial damage after X irradiation, role in radiosensitivity difference between L5178Y-R and L5178Y-S cells (mouse), **115**, 550

repair after X irradiation, role in radiosensitivity difference between L5178Y-R and L5178Y-S cells (mouse), **115**, 566

## damage

induced by uv irradiation, effect of cellular differentiation on repair (mouse), **116**, 217

induction and repair in  $\gamma$ -irradiated lymphoblasts, effects of oxygen and misonidazole (human), **115**, 436

in irradiated epithelial teratocarcinoma cells, comparison with V79 cells (human), **113**, 278

## double-strand breaks

induction and rejoining in cervical carcinoma cells of differing radiosensitivity after  $\gamma$  irradiation (human), **116**, 526

## repair

in eukaryotic cells with different radiosensitivities (*Trichoplusia ni*, V79 cells), **113**, 268

in  $\gamma$ -ray-sensitive XR-1 cells, cell cycle dependence, **115**, 325

inhibition by SR-4077 (CHO cells), **113**, 346; *erratum*, **114**, 643

resultant exponential or shouldered survival curves, dependence on postirradiation conditions (yeast), **114**, 54

X-ray-induced, measurement by neutral filter elution: calibration by  $^{125}\text{I}$  decay (V79 cells), **115**, 624

interaction with glutathione and other low-molecular-weight thiols: evidence for counterion condensation and coion depletion near DNA, **114**, 3

irradiated with  $\gamma$  or uv rays, cleavage by *Micrococcus luteus*  $\gamma$ -endonuclease, analysis, **114**, 556

nuclear, supercoiling, interactive effects of heat and  $\gamma$  irradiation (HeLa cells), **116**, 114

processing at nuclear matrix, blockage by hyperthermia (HeLa cells), **115**, 258

-protein crosslinks, repair in  $\gamma$ -irradiated V79 cells, effects of glutathione depletion and hypoxia, **116**, 89

radioprotection by thiols, relationship to thiol net charge, **114**, 11

redoxo-endonuclease-mediated cleavage at sites of uv-induced photoproducts, wavelength dependence (human), **113**, 543

repair patches, normal and xeroderma pigmentosum fibroblasts, proximity to persistent pyrimidine dimers, analysis (human), **116**, 245

selective  $^{125}\text{I}$  irradiation during cell cycle, effects on cell progression (CHO cells), **116**, 283

simian virus 40,  $\gamma$  irradiation and subsequent cell infection: intracellular induction and repair of strand breaks, analysis (CC91, CV-1 cells), **116**, 462

## single-strand breaks

$\gamma$ -ray-induced, radioprotective effects of WR-1065 (CHO cells), **113**, 155

induction in fibroblasts by solar uv irradiation, analysis (human skin), **116**, 313

induction and rejoining in jejunal cells, effects of radioprotectants WR-2721 and WR-1065 *in vivo* (mouse), **114**, 268

## strand breaks

and 1- $\beta$ -D-arabinofuranosylcytosine detectable sites induced by X and  $\gamma$  irradiation, comparison (human), **114**, 168

calculation from average doses to small doses, comments, **114**, 192

hyperthermic induction, role of poly(ADP-ribose)polymerase (HeLa cells), **116**, 406

induction and rejoining in AA8 cells and radiosensitive clones after  $\gamma$  irradiation, **116**, 511

X-ray-induced, cell cycle effect, comparison (murine mammary tumor cells), **116**, 228

## DNA polymerase

heat-induced loss in CHO cells, acid-induced increase, role of intracellular and extracellular pH, **115**, 576

## DNA synthesis

in CHO cells, heat effects, assessment of subsequent recovery, **114**, 125

delay in initiation after irradiation, effect of oxygen (murine melanoma), **113**, 102

## in lens epithelial cells

after irradiation with single and fractionated doses of X rays and neutrons, comparison (mouse), **114**, 567

stimulated from quiescence, sensitivity to X-ray-induced growth arrest (rat), **113**, 133

## Dosage

limited range, in repeated  $\beta$  irradiation of skin, 100% tumor induction (mouse), **115**, 488

lung X irradiation, effects on changes in collagen isotypes I, III, and IV (mouse), **115**, 515

in radiotherapy of patients with cervical cancer, relationship to second cancer risk, **116**, 3

## Dose fractionation

neutron, effect on oncogenic transformation of fibroblasts (mouse), **114**, 589; *erratum*, **116**, 550

X-ray, sensitivity of hepatocyte clonogens (mouse), **113**, 51

## Dose rate

effects on  $\gamma$ -irradiated normal and malignant cells, *in vitro* analysis (human), **114**, 415

low, effect on recovery of  $\gamma$ -irradiated hemopoietic and stromal progenitor cells in bone marrow (mouse), **115**, 481

very low,  $\gamma$  irradiation, mutation induction in leukemia cells (mouse), **115**, 273

## Dose-response relationships

in irradiation of amino acids, letter to the editor, **111**, 374; reply, **116**, 547

prenatal X irradiation effects on appearance of reflexes and physiologic markers (rat), **116**, 416

split-dose sparing of  $\gamma$ -ray-induced pulmonary endothelial dysfunction (rat), **114**, 627

thresholds in radiation exposure responses, letter to editor, **116**, 172

## Dose-spread kernels

and attenuation coefficients, relationships, **113**, 235

## Dosimetry

changes in, effect on cancer mortality risk estimates in atomic bomb survivors, **114**, 437

local,  $^{226}\text{Ra}$  in trabecular bone after iv injection (dog), **116**, 263

low-dose-rate irradiation of V79 cells: radiosensitivity enhancement by moderate hyperthermia, **114**, 379

micro, *see* Microdosimetry

neutron and  $\gamma$  irradiation, effects of 60 once-weekly exposures, **115**, 347

thermal, assessment for normal muscle and adipose tissues (pig), **114**, 225

## thermoluminescence

$\gamma$  doses from atomic bombs in Hiroshima and Nagasaki, reassessment, **113**, 1

measurements of  $\gamma$  radiation from atomic bomb at Hiroshima by predose technique, **113**, 227

very small doses per fraction of X or neutron radiation, effect on kidney (mouse), **114**, 385

## Droperidol

effect on tumor blood flow (rat), **114**, 64

with Fentanyl, effect on tumor blood flow (rat), **114**, 64

## E

## Editorial

guest, thresholds in radiation exposure responses, **114**, 1

## Electron nuclear double resonance and ESR spectroscopy

GMP single crystals X-irradiated at 10° K, **116**, 196

secondary radical formation and reaction mechanisms in X-irradiated single crystals of guanine hydrochloride monohydrate, **116**, 379

## Electrons

low-energy, in polyatomic gases, mean energy required for ion pair formation, **115**, 213

penetration, multiple scattering analysis, **115**, 26

subexcitation, absolute scattering probabilities in condensed water, determination, **114**, 467

## Electron scattering

absolute probabilities for subexcitation electrons in condensed water, determination, **114**, 467

multiple, analysis of penetration, **115**, 26

## Electron spin resonance

in analysis of radicals generated in X-irradiated L- $\alpha$ -amino-*n*-butyric acid HCl containing 1.5% L-cysteine HCl, **116**, 373

## and ENDOR spectroscopy

GMP single crystals X-irradiated at 10° K, **116**, 196

secondary radical formation and reaction mechanisms in X-irradiated single crystals of guanine hydrochloride monohydrate, **116**, 379

spin-trapping study of H<sub>2</sub>O<sub>2</sub> photolysis,  $\gamma$  radiolysis, and sonolysis of pyrimidine derivatives in aqueous solutions, **116**, 56

## Embryo

preimplantation, X - ray - induced nonlethal changes, assay with embryo aggregation chimeras (mouse), **113**, 289

## Emesis

$\gamma$ -radiation-induced, effects of zacopride (rhesus monkey), **115**, 595

## radiation-induced

characterization (ferret), **114**, 599

effect on local cerebral blood flow (ferret), **114**, 537

 $\gamma$ -Endonuclease

*Micrococcus luteus*, cleavage of  $\gamma$ - or uv-irradiated DNA, analysis, **114**, 556

ENDOR, *see* Electron nuclear double resonance

## Endothelial cells

- aortic, cell cycle progression after  $\gamma$  irradiation, analysis (bovine), **116**, 364
- capillary, hyperthermia effect *in vivo* (mouse), **114**, 297
- pulmonary, dysfunction after hemithorax exposure to  $\gamma$  rays, split-dose sparing (rat), **114**, 627
- umbilical cord vein, response to  $\gamma$  irradiation, *in vitro* analysis (human), **114**, 415

## Energy status

- cellular, effect of extracellular pH: relationship to hyperthermic sensitivity (CHO cells), **116**, 305

## Epidemiology

- cataract incidence in patients injected with  $^{224}\text{Ra}$ , **115**, 238

## Epithelial cells

- alveolar type 2, replicative activity, enhancement by methylprednisolone in radiation pneumonitis (mouse), **115**, 543
- lens, recovery from single and fractionated doses of X rays and neutrons, comparison (mouse), **114**, 567

## Ergothioneine

- radioprotection of bacteriophages T4 and P22 against  $\gamma$  irradiation inactivation, **114**, 319

## Erythrocytes

- protein shedding after microwave irradiation, chromatographic analysis (human), **114**, 500

ESR, *see* Electron spin resonance

## Etomidate

- effect on
  - RIF-1 tumor radiosensitivity (mouse), **114**, 105
  - tumor blood flow (rat), **114**, 64

## Eukaryotes

- wild-type, and *Escherichia coli*, uv action spectra (254–320 nm), comparison, **114**, 307

## Eye

- lens epithelial cells stimulated from quiescence, sensitivity to X-ray-induced growth arrest (rat), **113**, 133

## F

## Fentanyl

- with fluanisone or droperidol, effect on tumor blood flow (rat), **114**, 64

## Fibroblasts

- dermal
  - collagen biosynthesis,  $\gamma$ -ray-induced increases, 48-week study (mouse), **116**, 145
  - DNA single-strand breaks induced by solar uv irradiation, analysis (human), **116**, 313

- DNA strand breaks and 1- $\beta$ -D-arabinofuranosyl-cytosine detectable sites induced by X and  $\gamma$  irradiation, comparison (human), **114**, 168
- in exponential growth phase, correlation between survival curve and potentially lethal damage repair capacity (human), **116**, 74
- intracellular  $\text{Ca}^{2+}$  levels and inositol lipid metabolism, effects of hyperthermia (BALB/c 3T3 mouse, Chinese hamster), **113**, 414
- normal and xeroderma pigmentosum, DNA, proximity of repair patches to persistent pyrimidine dimers, analysis (human), **116**, 245
- oncogenic transformation by fractionated doses of neutrons, analysis (mouse), **114**, 589; *erratum*, **116**, 550

- radiosensitivity, enhancement by moderate hyperthermia at low  $^{137}\text{Cs}$  irradiation dose rates (Chinese hamster), **114**, 379

- repair of X-ray-induced potentially lethal damage, metabolic effects of cordycepin and 2-halo derivatives (Chinese hamster), **114**, 231
- response to  $\gamma$  irradiation, *in vitro* analysis (human lung, skin), **114**, 415

- sensitivity to acute uv exposures, alteration by multiple small far- or mid-uv light exposures, measurement by cell lethality and mutagenesis (Chinese hamster), **114**, 248

## Filter elution

- neutral, in measurement of X-ray-induced DNA double-strand breaks: calibration by  $^{125}\text{I}$  decay (V79 cells), **115**, 624

## Fluanisone

- with Fentanyl, effect on tumor blood flow (rat), **114**, 64

## Formate ions

- protective effects on radiation-induced inactivation of isolated transcriptionally active chromatin: influence of secondary radicals (*Tetrahymena*), **114**, 28

## G

## Gamma irradiation

- AA8 cells and radiosensitive clones
  - DNA strand break induction and rejoining, **116**, 511
  - survival and recovery, **115**, 223
- adenosine 5'-monophosphate, oxygen dependence of product formation, **113**, 447
- aortic endothelial cells, effect on cell cycle progression (bovine), **116**, 364
- bacteriophages T4 and P22, induced inactivation, radioprotective effects of ergothioneine, histidine, carnosine, and anserine, **114**, 319

- bone marrow, recovery of hemopoietic and stromal progenitor cells, effect of low dose rate (mouse), **115**, 481
- brain, associated blood flow changes, analysis in glioma model (rat), **115**, 586
- C57Bl mouse, single and fractionated doses, life-shortening and disease incidence, **113**, 300
- cell hybrids, induced expression of tumor-specific antigen, analysis (human), **114**, 84
- cervical carcinoma cells of differing radiosensitivity, DNA double-strand break induction and rejoining (human), **116**, 526
- CHO cells, induction of DNA single-strand breaks, radioprotective effects of WR-1065, **113**, 155
- continuous long-term, diploid yeast culture, associated mitotic recombination, **113**, 71
- DNA, subsequent cleavage by *Micrococcus luteus*  $\gamma$ -endonuclease, analysis, **114**, 556
- dosages from atomic bombs in Hiroshima and Nagasaki, reassessment, **113**, 1
- epithelial teratocarcinoma cells, DNA damage and survival parameters, comparison with V79 cells (human), **113**, 278
- Escherichia coli*  
radioprotection by cysteamine, mechanisms, **114**, 550  
*thyA* mutants, effects of dihydrothymine and thymine glycol on pyrimidine salvage and thymineless radiosensitization, **115**, 617
- fibrosarcoma, radiosensitivity of late recurrences (mouse), **113**, 334
- HeLa cells, and heat exposure, interactive effects on nuclear DNA supercoiling, **116**, 114
- hemithorax  
induced lung injury, serum copper levels as index, evaluation (rat), **114**, 613  
induced pulmonary endothelial dysfunction, split-dose sparing (rat), **114**, 627
- hepatocytes, comparative radiosensitivity (human, rat), **115**, 152
- hind thigh, tissue repair and repopulation in tumor bed effect (mouse), **114**, 621
- human cell lines, induction of DNA strand breaks and 1- $\beta$ -D-arabinofuranosylcytosine detectable sites, **114**, 168
- induced emesis, characterization (ferret), **114**, 599
- induced hypothermia, opposite effects of WR-2721 and WR-1065: correlation with oxygen uptake (guinea pig), **114**, 240
- induced temperature responses, role of prostaglandins and histamine H<sub>1</sub> and H<sub>2</sub> receptors (rat), **114**, 42
- jejunum, radioprotection by WR-2721 and WR-1065 *in vivo*: effects on DNA strand break induction and rejoining (mouse), **114**, 268
- kidney, subsequent characterization of abnormal nuclei in proximal tubular cells (mouse), **115**, 161
- leukemia cells at very low dose rate, mutation induction (mouse), **115**, 273
- limb bud cells *in vitro*, effects on chondrogenic development (chicken embryo), **116**, 356
- lung, induced pneumonitis, replicative activity of alveolar type 2 cells, enhancement by methylprednisolone (mouse), **115**, 543
- lymphoblasts, induction and repair of DNA damage, effects of oxygen and misonidazole (human), **115**, 436
- lymphocytes, chromosomal aberrations induced by acute and fractionated exposure, time dependence (human, monkey), **116**, 254
- mice  
effects of 60 once-weekly exposures, **115**, 347  
tumor induction: relative risk extrapolation across mouse strains and to man, **114**, 331  
-neutron irradiation, whole-body, radioprotection with WR-2721 and/or 16,16-dimethylprostaglandin E<sub>2</sub> (mouse), **115**, 605
- normal and malignant cells *in vitro*, analysis of radiation response characteristics (human), **114**, 415
- peripheral blood lymphocytes, interspecific cytogenetic comparison of responses (human, mouse), **115**, 334
- prenatal, effects on developing immune system (dog), **115**, 472
- simian virus 40, and subsequent cell infection: intracellular induction and repair of DNA strand breaks, analysis (CC91, CV-1 cells), **116**, 462
- thorax, induction of  
collagen biosynthesis increases: 48-week study in skin and skin fibroblast cultures (mouse), **116**, 145  
pneumonitis, protective effects of corticosteroids (mouse), **113**, 112
- thymus, effects on nonlymphoid components *in vitro* (dog), **115**, 84
- TN-368 cells, recovery enhancement by split-dose treatment, **115**, 413
- tumor cells, radiocurability, effects of *N*-methylformamide (mouse), **113**, 199
- in utero* and postpartum treatments, assessment of prenatal and early postnatal mortality (dog), **115**, 70



- V79 cells  
 effect on sensitivity to *N*-methyl-*N*-nitro-*N*-nitrosoguanidine, **115**, 609  
 induction of chromosome damage, radioprotective effects of WR-1065, **113**, 145  
 subsequent repair of chromatin damage, effects of glutathione depletion and hypoxia, **116**, 89  
 and treatment with hypertonic phosphate-buffered saline: estimation of interaction function  $\gamma(x)$ , **116**, 472
- whole-body  
 induced emesis, effects of zacopride (rhesus monkey), **115**, 595  
 subsequent regenerative effects of tetrachlorodecaoxide (rat), **115**, 115
- XR-1 cells, cell cycle-dependent repair of potentially lethal damage, **115**, 325
- Gamma radiation  
 from atomic bomb at Hiroshima, thermoluminescence dosimetry by predose technique, **113**, 227
- Gases  
 polyatomic, low-energy photons and electrons in, mean energy required for ion pair formation, **115**, 213
- Gibbs clip  
 effectiveness in RIF-1 tumor treatment, evaluation (mouse), **114**, 105
- Glucose  
 deprived hypoxic HeLa cells, hyperthermic killing, protection by purine ribonucleosides, **116**, 337
- Glutathione  
 acute depletion by L-buthionine sulfoximine and dimethylfumarate, toxic effects on mammary carcinoma cells (mouse), **114**, 215  
 content in colon tumor cells, changes after exposure to sodium butyrate (human), **114**, 579  
 depletion in  
 mitochondria, relationship to thermal sensitivity (CHO cells), **115**, 461  
 V79 cells, effect on repair of radiation-induced chromatin damage, **116**, 89  
 interaction with DNA: evidence for counterion condensation and coion depletion near DNA, **114**, 3  
 oxidation in CHO cells by SR-4077, **113**, 346; *erratum*, **114**, 643
- Glutathione disulfide  
 microinjection into CHO cells, induction of thermotolerance, **115**, 202
- Growth factors  
 mitogenic response of CHO HA-1 cells after hyperthermic cell killing, **113**, 501
- Guanine hydrochloride monohydrate  
 single crystals, X irradiation, formation of secondary radicals, reaction mechanisms, ESR and ENDOR spectroscopy, **116**, 379
- Guanosine 5'-monophosphate  
 single crystals X irradiated at 10° K, ESR/ENDOR study, **116**, 196
- H
- Heart  
 radiation-induced cardiomyopathy, analysis (dog), **113**, 120
- Heat-shock proteins  
 role of Ca<sup>2+</sup>, symposium introduction, **113**, 401  
 role in proliferation of synchronized neuroblastoma cells after heat treatment (mouse), **113**, 252  
 synthesis  
 in cells and tissues, relationship to intracellular free Ca<sup>2+</sup> levels (*Drosophila melanogaster*), **113**, 402  
 regulation in heat-resistant variants of CHO HA-1 cells, analysis, **116**, 427
- Heavy ions  
 high-energy, microdosimetry near trajectory, analysis, **116**, 183
- HeLa cells  
 DNA processing at nuclear matrix, blockage by hyperthermia, **115**, 258  
 glucose-deprived hypoxic, hyperthermic killing, protection by purine ribonucleosides, **116**, 337  
 heat sensitivity  
 effect of pentamidine, **116**, 320  
 role of poly(ADP-ribose)polymerase, **116**, 406  
 intracellular Ca<sup>2+</sup> levels and inositol lipid metabolism, effects of hyperthermia, **113**, 414  
 nuclear DNA supercoiling, interactive effects of  $\gamma$  irradiation and heat, **116**, 114
- Hepatocytes  
 clonogens, sensitivity to X-ray dose fractionation (mouse), **113**, 51  
 colony-forming ability and chromosomal injury, long-term repair *in vivo* after X irradiation (mouse), **113**, 40  
 radiosensitivity, comparison between human and rat, **115**, 152
- Hiroshima  
 atomic bombs,  $\gamma$  doses, reassessment, **113**, 1  
 $\gamma$  radiation from atomic bomb, thermoluminescence dosimetry measurements by predose technique, **113**, 227
- Histamine receptors  
 H<sub>1</sub> and H<sub>2</sub>, role in irradiation-induced temperature responses (rat), **114**, 42

- Histidine**  
radioprotection of bacteriophages T4 and P22 against  $\gamma$  irradiation inactivation, **114**, 319
- Hodgkin's disease**  
radiotherapy of affected patient, induction of structural chromosome aberrations in peripheral lymphocytes, **114**, 528
- Hydralazine**  
reduction of tumor blood flow after X irradiation, effect on efficacy of misonidazole and RSU-1069 (mouse), **115**, 292
- Hydrogen**  
abstraction from sugar moiety by thymine radicals in oligo- and polydeoxynucleotides, analysis, **116**, 210
- Hydrogen peroxide**  
resistant variants, increase in catalase activity (CHO HA-1 cells), **114**, 114
- 8-Hydroxyadenosine 5'-monophosphate**  
formation in  $\gamma$ -irradiated adenosine 5'-monophosphate solutions, role of oxygen, **113**, 447
- Hydroxyl radicals**  
various scavengers, protective effects on radiation-induced inactivation of isolated transcriptionally active chromatin: influence of secondary radicals (*Tetrahymena*), **114**, 28
- 8-Hydroxyquinoline**  
in tumor-targeted cell killing, evaluation (mouse), **115**, 373
- Hyperthermia**  
associated cell killing, and mitogenic response to serum and growth factors, relationship (CHO HA-1 cells), **113**, 501  
blockage of DNA processing at nuclear matrix (HeLa cells), **115**, 258  
cell killing of synchronous G1 and S phase CHO cells *in vitro*, time-temperature analysis, **113**, 318  
CHO cells at 45°C  
development of thermotolerance after microinjection with glutathione disulfide, **115**, 202  
at pH 6.6  
development of thermotolerance and changes in intracellular pH, **115**, 106  
relationship between intra- and extracellular pH, **115**, 96  
combined with 8-hydroxyquinoline treatment, in tumor-targeted cell killing, evaluation (mouse), **115**, 373  
effect on  
DNA synthesis, assessment of subsequent recovery (CHO cells), **114**, 125  
intracellular  $\text{Ca}^{2+}$  and inositol lipid metabolism (mammalian cells), **113**, 414  
X-ray-induced carcinogenesis (mouse), **115**, 448  
and  $\gamma$  irradiation, interactive effects on nuclear DNA supercoiling (HeLa cells), **116**, 114  
graduated doses, responses of normal muscle and adipose tissues (pig), **114**, 225  
induced cell death of plateau-phase CHO cells, analysis of rapid and slow modes, **116**, 157  
induced cell injury, role of  $\text{Ca}^{2+}$ , symposium introduction, **113**, 401  
induced heat-shock protein synthesis, regulation in heat-resistant variants of CHO HA-1 cells, **116**, 427  
induced mitochondrial damage in CHO cells, electron microscopic analysis, **115**, 421  
induced radiosensitization of CHO cells, acid-induced increase, role of intracellular and extracellular pH, **115**, 576  
induction of  $\text{Ca}^{2+}$ -dependent processes, role in thermoresistance (Chinese hamster lung, Morris hepatoma cells), **113**, 426  
inhibition of potentially lethal radiation damage repair in normal hamster cells, mouse cells, and transformed mouse cells, **113**, 171  
irradiation-induced, role of prostaglandins and histamine  $\text{H}_1$  and  $\text{H}_2$  receptors (rat), **114**, 42  
moderate, enhancement of V79 cell radiosensitivity at low  $^{137}\text{Cs}$  irradiation dose rates, **114**, 379  
radiofrequency-induced, *in vivo* inhibition of capillary angiogenesis (mouse), **114**, 297  
selective killing of glucose-deprived hypoxic HeLa cells, protection by purine ribonucleosides, **116**, 337  
sensitivity of  
CHO cells, relationship to extracellular pH effects on intracellular pH and cell energy status, **116**, 305  
HeLa cells  
effect of pentamidine, **116**, 320  
role of poly(ADP-ribose)polymerase, **116**, 406  
V79 cells, role of poly(ADP-ribose)synthetase, **116**, 442  
sensitization of CHO cells to, role of low intracellular pH, **114**, 154  
and serum starvation, effect on viability of CHO HA-1 cells, **113**, 513  
and starvation conditions, effects on radiosensitivity and repair of potentially lethal and sublethal damage in L5178Y-R and L5178Y-S cells, **113**, 458

- treatment of synchronized neuroblastoma cells, subsequent proliferation, role of heat-shock proteins (mouse), **113**, 252
- and X irradiation, intestine, induction of thermotolerance, effect on time-temperature relationships (mouse), **113**, 375
- Hypothermia**
- $\gamma$ -ray-induced, opposite effects of WR-2721 and WR-1065, correlation with oxygen uptake (guinea pig), **114**, 240
- irradiation-induced, role of prostaglandins and histamine H<sub>1</sub> and H<sub>2</sub> receptors (rat), **114**, 42
- Hypoxia**
- effects on repair of radiation-induced chromatin damage in V79 cells, **116**, 89
- postirradiation, enhancement of tumor cell radiosensitivity: time course and oxygen concentration dependency (hamster, human, mouse), **116**, 124
- RIF-1 tumor, effect of treatment with etomidate and Gibbs clip, evaluation (mouse), **114**, 105
- I
- Imaging**
- NMR, central nervous system after heavy ion irradiation (rat), **113**, 79
- Immune responses**
- alterations in prenatal dogs after  $\gamma$  irradiation, **115**, 472
- atomic bomb survivors in Hiroshima, assessment, **116**, 343
- Infection**
- postirradiation, local and systemic, management with antibiotics, review, **115**, 1
- Injury**
- chronic pulmonary, induced by <sup>239</sup>PuO<sub>2</sub> inhalation, effect on cardiopulmonary function (dog), **114**, 314
- Interaction function  $\gamma(x)$**
- for V79 cells treated with hypertonic phosphate-buffered saline after  $\gamma$  or X irradiation, estimation, **116**, 472
- Intestine**
- jejunum, *in vivo* radioprotection by WR-2721 and WR-1065: effects on DNA strand break induction and rejoining (mouse), **114**, 268
- preirradiated, thermotolerance, effect on time-temperature relationships (mouse), **113**, 375
- Iodine**
- <sup>125</sup>I
- decay calibration in labeled DNA for measurement of X-ray-induced double-strand breaks by neutral filter elution (V79 cells), **115**, 624
- selective irradiation of DNA during cell cycle, effects on cell progression (CHO cells), **116**, 283
- Ionizing irradiation**
- bilateral thoracic, associated early structural changes in lung, analysis (sheep), **114**, 138
- central nervous system, subsequent NMR imaging and spectroscopy (rat), **113**, 79
- colon tumor cells, radiosensitivity, effects of  $\alpha$ -difluoromethylornithine-induced polyamine depletion (human), **114**, 634
- DNA, induced double-strand breaks, repair, resultant exponential or shouldered survival curves, dependence on postirradiation conditions, **114**, 54
- fibrosarcoma
- associated changes in bromodeoxyuridine labeling index (mouse), **116**, 453
- proliferation kinetics during fractionated treatment (mouse), **116**, 327
- induced emesis, effect on local cerebral blood flow (ferret), **114**, 537
- induced inactivation of isolated transcriptionally active chromatin, protection by OH scavengers: influence of secondary radicals (*Tetrahymena*), **114**, 28
- melanoma cells, delay in initiation of DNA synthesis, effect of oxygen (mouse), **113**, 102
- normal and postremectomized cats, radioemetic protection 24 hours after exposure, analysis, **114**, 77
- r-chromatin *in vitro*, induced inactivation, sulfhydryl protection and oxygen effect, influence of *t*-butanol (*Tetrahymena*), **115**, 141
- Salmonella typhimurium*, induction of *his*<sup>+</sup> reversions, comparative analysis of different radiation types, **116**, 292
- thorax, induced cardiomyopathy, analysis (dog), **113**, 120
- V79 cells, low dose rates: enhancement of radiosensitivity by moderate hyperthermia, **114**, 379
- water ice pulsed with 0.53-MeV electrons, red luminescence emission, **115**, 403
- Ionizing radiation**
- high-LET particles, simulated linear track structures, frequency distributions and density functions of distances, **113**, 437
- induced local and systemic infections, management with antibiotics, review, **115**, 1
- quality factor, redefinition as function of lineal energy, **114**, 480
- Ion pairs**
- formation, required mean energy, measurement for low-energy photons and electrons in polyatomic gases, **115**, 213

## K

- Kerma factor  
 carbon, for 14.6-MeV neutrons, calorimetric measurements, correction, **113**, 396; reply, **113**, 398
- Ketamine  
 with xylazine or midazolam, effect on tumor blood flow (rat), **114**, 64
- Kidney  
 $\gamma$  irradiation, subsequent characterization of abnormal nuclei in proximal tubular cells (mouse), **115**, 161  
 response to very small doses per fraction of X or neutron radiation (mouse), **114**, 385

## L

- Lens  
 cataract formation, incidence in patients injected with  $^{224}\text{Ra}$ , epidemiological analysis, **115**, 238
- Lesions  
 area postrema, chronic, effect of radioemetic protection at 24 hours (cat), **114**, 77
- Leukotrienes  
 induction of radioprotection of hematopoietic stem cells (mouse), **113**, 388
- Life span  
 reduction in C57Bl mouse after single and fractionated  $\gamma$  and neutron irradiations, **113**, 300  
 shortening in  
 BC3F<sub>1</sub> mice after low-dose neutron and X irradiation, **113**, 362  
 B6CF<sub>1</sub> mice after neutron and  $\gamma$  irradiation, effects of 60 once-weekly exposures, **115**, 347
- Lineal energy  
 in ionizing radiation, relationship to quality factor, **114**, 480
- Lonidamine  
 inhibition of cellular oxygen utilization (CHO, FSa-II cells), **113**, 356
- Luminescence  
 red emission from electron-pulsed water ice, **115**, 403
- Lung  
 alveolar type 2 cells, replicative activity, enhancement by methylprednisolone in radiation pneumonitis (mouse), **115**, 543  
 carcinogenesis, promotion by plutonium particle aggregation after  $^{239}\text{PuO}_2$  inhalation (rat), **116**, 393  
 chronic  $^{239}\text{PuO}_2$  inhalation injury, effect on cardiopulmonary function (dog), **115**, 314

- collagen isotypes I, III, and IV, changes after X irradiation, effects of time, dose, and WR-2721 (mouse), **115**, 515
- early structural changes after thoracic irradiation, analysis (sheep), **114**, 138
- endothelial dysfunction after hemithorax exposure to  $\gamma$  rays, split-dose sparing (rat), **114**, 627
- injury after hemithorax exposure to  $\gamma$  rays, serum copper levels as index, evaluation (rat), **114**, 613
- metastases of B16<sub>a</sub> melanoma, comparative effects of daily and weekly fractions of X irradiation (mouse), **114**, 354
- Lymphoblasts  
 $\gamma$ -irradiated, induction and repair of DNA damage, effects of oxygen and misonidazole (human), **115**, 436  
 L5178Y-R and L5178Y-S leukemic, difference in radiosensitivity, role of DNA and chromosome repair (mouse), **115**, 566  
 initial DNA and chromosome damage (mouse), **115**, 550
- Lymphocytes  
 chromosomal aberrations induced by acute and fractionated  $\gamma$  irradiation, time dependence (human, monkey), **116**, 254  
 peripheral blood  
 in Hodgkin's disease patient, structural chromosome aberrations induced by radiotherapy, **114**, 528  
 responses to  $\gamma$  irradiation, interspecific cytogenetic comparison (human, mouse), **115**, 334
- Lymphoid organs  
 total X irradiation, late somatic effects (mouse), **116**, 503

## M

- Mechlorethamine  
 and X irradiation, quantitative aspects of interactive killing effects in bacteria, **115**, 124
- Membranes  
 thymic, cytoplasmic and nuclear, conformational changes after microwave exposure (rabbit), **115**, 44
- 2-Mercaptoethanol  
 protection against radiation-induced inactivation of r-chromatin *in vitro*, effect of *t*-butanol (*Tetrahymena*), **115**, 141
- Metastases  
 pulmonary, B16<sub>a</sub> melanoma, comparative effects of daily and weekly fractions of X irradiation (mouse), **114**, 354

- Methanol  
protective effects on radiation-induced inactivation of isolated transcriptionally active chromatin: influence of secondary radicals (*Tetrahymena*), **114**, 28
- Methoxyflurane  
effect on tumor blood flow (rat), **114**, 64
- N*-Methylformamide  
effect on  
oxygen enhancement ratio of colon tumor cells (human), **113**, 191  
radiocurability of tumor cells (mouse), **113**, 199
- N*-Methyl-*N'*-nitro-*N*-nitrosoguanidine  
V79 cell sensitivity to, effect of  $\gamma$  preirradiation, **115**, 609
- Methylprednisolone  
enhancement of alveolar type 2 cell replicative activity in radiation pneumonitis (murine lung), **115**, 543  
protective effect on radiation pneumonitis (mouse), **113**, 112
- Microdosimetry  
application in radiobiology, **113**, 15  
near trajectory of high-energy heavy ions, analysis, **116**, 183  
0.3–20-MeV proton track structures obtained bycomputer simulation, **115**, 389
- Microwave irradiation  
erythrocytes, induction of protein shedding, chromatographic analysis (human), **114**, 500  
thymus, effect on cellular functional state (rabbit), **115**, 44
- Midazolam  
alone and with ketamine, effect on tumor blood flow (rat), **114**, 64
- Misonidazole  
effects on induction and repair of DNA damage in  $\gamma$ -irradiated lymphoblasts (human), **115**, 436  
plus photons, in fractionated irradiation of spontaneous tumors, therapeutic gain factors (mouse), **116**, 482  
radiosensitization of tumor cells, enhancement by hydralazine-induced hypoxia after X irradiation (mouse), **115**, 292
- Mitochondria  
damage in CHO cells exposed to hyperthermia, electron microscopic analysis, **115**, 421  
glutathione depletion, relationship to thermal sensitivity (CHO cells), **115**, 461
- Models  
mathematical, subpopulation exclusion in heterogeneous neoplasms caused by tumor bed effect-induced environmental stress, **115**, 533
- Mortality  
cancer-induced, risk estimates in atomic bomb survivors, effect of changes in dosimetry, **114**, 437  
prenatal and early postnatal, assessment after *in utero* and postpartum exposure to  $\gamma$  radiation (dog), **115**, 70
- Muscle  
normal, response to graduated doses of hyperthermia (pig), **114**, 225
- Mutagenesis  
V79 cells after acute exposures, effects of multiple small far- or mid-uv light exposures, **114**, 248
- Mutants  
heat-sensitive, thermotolerant defective CHO cells, isolation and characterization, **113**, 526
- Mutations  
in A<sub>L</sub> cells, induction by neutron irradiation, **115**, 281  
*his*<sup>+</sup> reversions in *Salmonella typhimurium*, induction by various types of ionizing radiation, comparative analysis, **116**, 292  
induced by *N*-methyl-*N'*-nitro-*N*-nitrosoguanidine, effect of  $\gamma$  preirradiation (V79 cells), **115**, 609  
in leukemia cells, induction by very low dose rate  $\gamma$  irradiation (mouse), **115**, 273
- N
- NAD<sup>+</sup> ADP-ribosyltransferase  
role in heat sensitivity of HeLa cells, **116**, 406
- Nagasaki  
atomic bombs,  $\gamma$  doses, reassessment, **113**, 1
- Natural killer cells  
activity against B16<sub>a</sub> melanoma, comparative effects of daily and weekly fractions of X irradiation (mouse), **114**, 354
- Neon ions  
and X rays, sequential exposure of fibroblasts: damage interaction effects as function of cell cycle stage (V79 cells), **115**, 54
- Neoplasms  
radiogenic, relative risk extrapolation across mouse strains and to man, **114**, 331
- Neurons  
cerebellar, chromatin structure, postirradiation alterations, analysis (rat), **114**, 94
- Neutron irradiation  
A<sub>L</sub> cells, mutation induction and relative biological effectiveness, **115**, 281

- BC3F<sub>1</sub> mouse, at low dosage, tumor induction and life-shortening, **113**, 362
- C57Bl mouse, single and fractionated doses, life-shortening and disease incidence, **113**, 300
- epithelial teratocarcinoma cells, DNA damage and survival parameters, comparison with V79 cells (human), **113**, 278
- fast, spontaneous tumors, therapeutic gain factors for fractionated treatment (mouse), **116**, 482
- fibroblasts, oncogenic transformation by fractionated doses, analysis (mouse), **114**, 589; *erratum*, **116**, 550
- $\gamma$  irradiation, whole-body, radioprotection with WR-2721 and/or 16,16-dimethylprostaglandin E<sub>2</sub> (mouse), **115**, 605
- kidney, response to very small doses per fraction, comparison to X irradiation (mouse), **114**, 385
- mice, effect of 60 once-weekly exposures, **115**, 347
- V79 cells, induction of chromosome damage, radioprotective effects of WR-1065, **113**, 145
- and X irradiation, lens epithelial cells, recovery from single and fractionated doses, comparison (mouse), **114**, 567
- whole-body, effects of graded doses on stromal compartment of thymus (mouse), **113**, 25
- Neutrons**
- 14.6-MeV, carbon kerma factor, calorimetric measurements, correction, **113**, 396; reply, **113**, 398
- Nitrogen mustard, *see* Mechlorethamine
- 1(2 - Nitro - 1 - imidazolyl) - 3 - (1 - aziridinyl) - 2 - propanol, *see* RSU-1069
- Nuclear accidents**
- treatment of victims, role of bone marrow transplantation, **113**, 205
- Nuclear magnetic resonance**
- <sup>31</sup>P, in analysis of pentobarbital anesthesia effects on tumor energy metabolism *in vivo* (mouse), **115**, 361
- Nuclear power plants**
- safety in the United States, assessment, **113**, 211, 217
- Nuclei**
- abnormal, in renal proximal tubular cells after  $\gamma$  irradiation, characterization (mouse), **115**, 161
- O**
- Obituary**
- Karl Günther Zimmer, **116**, 178
- Oligodeoxynucleotides
- sugar moiety, H atom abstraction by thymine radicals, analysis, **116**, 210
- Oxidation**
- thiols in CHO cells by SR-4077, **113**, 346; *erratum*, **114**, 643
- WR-1065, influencing factors, **113**, 243
- Oxygen**
- dependence of
- cytotoxic and radiosensitizing effects of cis-dichlorodiammineplatinum(II) on cervical carcinoma cells *in vitro* (human), **114**, 489
- product formation in  $\gamma$ -irradiated adenosine 5'-monophosphate solutions, **113**, 447
- radiosensitivity enhancement by postirradiation hypoxia (hamster, human, murine tumor cells), **116**, 124
- effect on
- delay in initiation of DNA synthesis after irradiation (murine melanoma), **113**, 102
- induction and repair of DNA damage in  $\gamma$ -irradiated lymphoblasts (human), **115**, 436
- radiation-induced inactivation of r-chromatin *in vitro*, influence of *t*-butanol (*Tetrahy-mena*), **115**, 141
- Oxygen enhancement ratio**
- colon tumor cells, effects of *N*-methylformamide and sodium butyrate (human), **113**, 191
- Oxygen uptake**
- in brain homogenates, relationship to opposite effects of WR-2721 and WR-1065 on  $\gamma$ -ray-induced hypothermia (guinea pig), **114**, 240
- by CHO and FSa-II cells, inhibition by lonidamine, **113**, 356
- P**
- Pentamidine**
- effect on heat sensitivity of HeLa cells, **116**, 320
- Pentobarbital**
- anesthesia, effects on tumor energy metabolism *in vivo*, analysis by <sup>31</sup>P NMR spectroscopy (mouse), **115**, 361
- effect on tumor blood flow (rat), **114**, 64
- pH**
- extracellular
- effects on intracellular pH and cell energy status: relationship to hyperthermic sensitivity (CHO cells), **116**, 305
- role in acid-induced increase in hyperthermic reagentsensitization (CHO cells), **115**, 576
- intracellular
- changes in CHO cells heated at 45°C at pH 6.6, **115**, 106

- low values, role in CHO cell sensitization to hyperthermia, **114**, 154  
relationship to extracellular pH of CHO cells heated at 45°C at pH 6.6, **115**, 96  
role in acid-induced increase in hyperthermic radiosensitization (CHO cells), **115**, 576
- Phosphoinositides**  
cellular metabolism, effect of hyperthermia (mammalian cells), **113**, 414
- Photolysis**  
ultraviolet, pyrimidine derivatives in aqueous solutions containing H<sub>2</sub>O<sub>2</sub>, spin-trapping study, **116**, 56
- Photons**  
low-energy, in polyatomic gases, mean energy required for ion pair formation, **115**, 213  
plus normobaric O<sub>2</sub>, hyperbaric O<sub>2</sub>, or misonidazole, in fractionated irradiation of spontaneous tumors, therapeutic gain factors (mouse), **116**, 482
- Plutonium**  
particle aggregation in lung after <sup>239</sup>PuO<sub>2</sub> inhalation, promotion of carcinogenesis (rat), **116**, 393  
<sup>239</sup>Pu, inhalation-induced chronic lung injury, effect on cardiopulmonary function (dog), **115**, 314
- Pneumonitis**  
γ-radiation-induced  
protective effect of corticosteroids (mouse), **113**, 112  
replicative activity of alveolar type 2 cells, enhancement by methylprednisolone (mouse), **115**, 543
- Poly(adenosinediphosphoribose)**  
synthesis inhibitors, and structurally related compounds, effects on X-irradiation-induced G<sub>2</sub> arrest (CHO cells), **113**, 58
- Poly(ADP-ribose)polymerase**, *see* NAD<sup>+</sup> ADP-riboseyltransferase
- Poly(ADP-ribose)synthetase**  
role in thermotolerance and heat and radiation responses (V79 cells), **116**, 442
- Polyamines**  
α - difluoromethylornithine - induced depletion, effects on radiosensitivity of colon carcinoma cells (human), **114**, 634
- Polydeoxynucleotides**  
sugar moiety, H atom abstraction by thymine radicals, analysis, **116**, 210
- Porfomycin**  
as adjunct to radiotherapy, preclinical studies (murine mammary tumor cells), **116**, 100
- Potentially lethal damage**  
α form, arabinofuranosyladenine-mediated fixation in X-irradiated plateau-phase CHO cells, relationship to chromosome repair, **114**, 361  
in γ-ray-sensitive XR-1 cells, cell cycle-dependent repair (Chinese hamster), **115**, 325
- repair**  
capacity of fibroblasts in exponential growth phase, correlation with survival curve (human), **116**, 74  
in γ-irradiated normal and malignant cells, *in vitro* analysis (human), **114**, 415  
and inhibition by hyperthermia in normal hamster cells, mouse cells, and transformed mouse cells, **113**, 171  
in V79 cells expressible by postirradiation treatment with hypertonic phosphate-buffered saline, analysis, **116**, 472  
in X-irradiated cerebral gliosarcoma cells grown as monolayers and spheroids, comparison (rat), **114**, 515  
and sublethal damage  
in L5178Y-R and L5178Y-S cells, effects of reduced temperature and starvation conditions, **113**, 458  
repair in L5178Y lymphoma cells differing in radiation sensitivity (mouse), **113**, 183  
X-ray-induced, in V79 cells, repair, metabolic effects of cordycepin and 2-halo derivatives, **114**, 231
- Proadipocytes**  
uv-irradiation-induced DNA damage, effect of cellular differentiation on repair (mouse), **116**, 217
- Proliferation**  
fibrosarcoma cells, kinetics during fractionated ionizing irradiation (mouse), **116**, 327
- Prostaglandins**  
role in irradiation-induced temperature responses (rat), **114**, 42
- Proteins**  
-DNA crosslinks, repair in γ-irradiated V79 cells, effects of glutathione depletion and hypoxia, **116**, 89  
erythrocyte, shedding after microwave irradiation, chromatographic analysis (human), **114**, 500  
heat-shock, *see* Heat-shock proteins
- Protein synthesis**  
in lens epithelial cells stimulated from quiescence, sensitivity to X-ray-induced growth arrest (rat), **113**, 133  
in X-irradiated CHO-tsH1 and CHO-SC1 cells, analysis, **114**, 281
- Protons**  
0.3-20-MeV, track structures obtained by computer simulation, microdosimetric aspects, **115**, 389

## Purine ribonucleosides

effect on hyperthermic killing of glucose-deprived hypoxic HeLa cells, **116**, 337

## Pyrimidine ribonucleosides

effect on hyperthermic killing of glucose-deprived hypoxic HeLa cells, **116**, 337

## Pyrimidines

derivatives in aqueous solutions, sonolysis, radiolysis, and hydrogen peroxide photolysis: spin-trapping study, **116**, 56

dimers, persistent, in DNA of normal and xeroderma pigmentosum fibroblasts, proximity to repair patches, analysis (human), **116**, 245

salvage, absence in *Escherichia coli thyA* cells fed dihydrothymine and thymine glycol, **115**, 617

## Q

## Quality factor

in ionizing radiation, redefinition as function of lineal energy, **114**, 480

## R

## Radiation

exposure responses, thresholds in, guest editorial, **114**, 1

galactic cosmic, transport codes, analytic benchmark solution, **114**, 201

linear energy transfer, thresholds in exposure responses, letter to editor, **116**, 172

low dose-rate exposures, importance of determination of effects, editorial, **116**, 1

research, multidisciplinary contributions of the journal, letter to the editor, **114**, 198

Radicals, *see also specific radicals*

carbon- and sulfur-centered, generated in X-irradiated L- $\alpha$ -amino-n-butyric acid HCl containing 1.5% L-cysteine HCl, ESR study, **116**, 373

secondary, formation and reaction mechanisms in X-irradiated single crystals of guanine hydrochloride monohydrate, ESR and ENDOR spectroscopy, **116**, 379

## Radiobiology

application of microdosimetry, **113**, 15

## Radiolabeling

DNA with  $^{125}\text{I}$ , decay calibration for measurement of X-ray-induced double-strand breaks (V79 cells), **115**, 624

## Radiolysis

aqueous solutions of pyrimidine derivatives, spin-trapping study, **116**, 56

pulse, in analysis of radicals produced from methylated uracils via  $\text{SO}_4^-$  oxidation, **114**, 207

## Radioprotection

bacteriophages T4 and P22 against  $\gamma$  irradiation inactivation, mediation by ergothioneine, histidine, carnosine, and anserine, **114**, 319

brain by WR-2721 via entry across modified blood-brain barrier (rat), **115**, 303

DNA by thiols, relationship to thiol net charge, **114**, 11

emesis, in normal and postremectomized cats at 24 hours after  $^{60}\text{Co}$  irradiation, analysis, **114**, 77

*Escherichia coli* by cysteamine, mechanisms, **114**, 550

hematopoietic stem cells, induction by leukotrienes (mouse), **113**, 388

jejunum by WR-2721 and WR-1065 *in vivo*: effects on DNA strand break induction and rejoining (mouse), **114**, 268

mice against neutron- $\gamma$  irradiation with WR-2721 and/or 16,16-dimethylprostaglandin  $\text{E}_2$ , **115**, 605

standards, need for good risk estimates, editorial, **116**, 1

V79 cells by WR-1065 after  $\gamma$ -ray- and fission-spectrum neutron-induced chromosome damage, **113**, 145

WR-1065 against  $\gamma$ -ray-induced DNA single-strand breaks in CHO cells, **113**, 155

## Radiosensitivity

CHO cells, effect of dimethylfumarate, **115**, 495

colon tumor cells

changes after exposure to sodium butyrate (human), **114**, 579

effects of  $\alpha$ -difluoromethylornithine-induced polyamine depletion (human), **114**, 634

DNA synthesis in lens epithelial cells exposed to X-ray-induced growth arrest after stimulation from quiescence (rat), **113**, 133

eukaryotic cells, variation among, effect on repair of DNA double-strand breaks (*Trichoplusia ni*, V79 cells), **113**, 268

fibroblasts in exponential growth phase, correlation with potentially lethal damage repair capacity, analysis (human), **116**, 74

fibrosarcoma late recurrences after radiotherapy (mouse), **113**, 334

hepatocytes, comparison between human and rat, **115**, 152

L5178Y lymphoma cells to X irradiation, repair of potentially lethal damage and sublethal damage (mouse), **113**, 183

L5178Y-R and L5178Y-S cells

differences in, role of

DNA and chromosome repair (mouse), **115**, 566



- initial DNA and chromosome damage (mouse), **115**, 550
- effects of reduced temperature and starvation conditions, **113**, 458
- normal and malignant cells exposed to  $\gamma$  rays *in vitro*, evaluation (human), **114**, 415
- RIF-1 tumor, effect of etomidate, **114**, 105
- role of poly(ADP-ribose)synthetase (V79 cells), **116**, 442
- thymus nonlymphoid components to  $\gamma$ -ray exposure *in vitro*, evaluation (dog), **115**, 84
- tumor cells
- assessment techniques, implications for clinical oncology (human), **114**, 401
  - enhancement by postirradiation hypoxia: time course and oxygen concentration dependency (hamster, human, mouse), **116**, 124
  - initial part of survival curve as predictor, evaluation (human), **114**, 425
- V79 cells
- acute uv exposures, alteration by multiple small far- or mid-uv light exposures, measurement by cell lethality and mutagenesis, **114**, 248
  - enhancement by moderate hyperthermia at low  $^{137}\text{Cs}$  irradiation dose rates, **114**, 379
- Radiosensitization
- cervical carcinoma cells by *cis*-dichlorodiammineplatinum(II), *in vitro* analysis (human), **114**, 489
- CHO cells
- by hyperthermia, acid-induced increase, role of intracellular and extracellular pH, **115**, 576
  - by SR-4077, **113**, 346; *erratum*, **114**, 643
- thymineless, prevention in *Escherichia coli thya* cells fed dihydrothymine and thymine glycol, **115**, 617
- tumors *in vivo* by diethyldithiocarbamate (mouse), **116**, 539
- Radiotherapy
- in conjunction with porfirimycin, preclinical studies (murine mammary tumor cells), **116**, 100
  - fractionated, outcome, initial part of survival curve as predictor, evaluation (human), **114**, 425
- Hodgkin's disease patient, induction of structural chromosome aberrations in peripheral lymphocytes, **114**, 528
- induced carcinogenesis in patients with cervical cancer: relationship between radiation dose and cancer risk, **116**, 3
- Radium
- $^{224}\text{Ra}$ , injected patients, incidence of cataracts, epidemiological analysis, **115**, 238
  - $^{226}\text{Ra}$ , microdistribution and local dosimetry in trabecular bone after iv injection (dog), **116**, 263
- Recombination
- mitotic, in diploid yeast strain after continuous long-term  $\gamma$  irradiation, **113**, 71
- Recovery
- AA8 cells and radiosensitive clones after  $\gamma$  irradiation, **115**, 223
  - hemopoietic and stromal progenitor cells in  $\gamma$ -irradiated bone marrow, effect of low dose rate (mouse), **115**, 481
  - split-dose, analysis in X-irradiated CHO-tsH1 and CHO-SC1 cells, **114**, 281
  - TN-368 cells after  $\gamma$  irradiation, enhancement by split-dose treatment, **115**, 413
  - tumor cells after X irradiation, effect of *N*-methylformamide (mouse), **113**, 199
- Redoxy-endonuclease
- mediated DNA cleavage at sites of uv-induced photoproducts, wavelength dependence (human), **113**, 543
- Relative biological effectiveness
- neutron irradiation of
    - A<sub>L</sub> cells, **115**, 281
    - mice, **115**, 347
- Repair
- chromosomes and DNA after X-ray-induced damage, role in radiosensitivity difference between L5178Y-R and L5178Y-S cells (mouse), **115**, 566
  - DNA double-strand breaks
    - in eukaryotic cells with different radiosensitivities (*Trichoplusia ni*, V79 cells), **113**, 268
    - in  $\gamma$ -ray-sensitive XR-1 cells, dependence on cell cycle phase, **115**, 325
    - inhibition by SR-4077 (CHO cells), **113**, 346; *erratum*, **114**, 643  - DNA lesions in  $\gamma$ -irradiated lymphoblasts, effects of oxygen and misonidazole (human), **115**, 436
  - long-term *in vivo*, colony-forming ability and chromosomal injury in X-irradiated hepatocytes (mouse), **113**, 40
  - potentially lethal damage
    - fibroblasts in exponential growth phase, correlation with survival curve (human), **116**, 74
    - and inhibition by hyperthermia in normal hamster cells, mouse cells, and transformed mouse cells, **113**, 171
    - and sublethal damage
      - in L5178Y lymphoma cells differing in radiation sensitivity (mouse), **113**, 183
      - in L5178Y-R and L5178Y-S cells, effects of reduced temperature and starvation conditions, **113**, 458

- Repair patches  
 in DNA of normal and xeroderma pigmentosum fibroblasts, proximity to persistent pyrimidine dimers, analysis (human), **116**, 245
- Resistance  
 hydrogen peroxide, associated increases in catalase activity (CHO HA-1 cells), **114**, 114
- Respiration  
 pulmonary, effect of chronic  $^{239}\text{PuO}_2$  inhalation exposure (dog), **115**, 314
- Retina  
 effect of accelerated argon ions (rat), **115**, 192
- Risk estimation  
 as basis for sane radiation protection standards, editorial, **116**, 1  
 radiotherapy-induced carcinogenesis in patients with cervical cancer, evaluation of broad dose range, **116**, 3
- RNA  
 synthesis in lens epithelial cells stimulated from quiescence, sensitivity to X-ray-induced growth arrest (rat), **113**, 133
- RSU-1069  
 radiosensitization of tumor cells, enhancement by hydralazine-induced hypoxia after X irradiation (mouse), **115**, 292
- S**
- Saline  
 hypertonic phosphate-buffered, treatment of V79 cells after  $\gamma$  or X irradiation: estimation of interaction function  $\gamma(x)$ , **116**, 472
- Salivary gland  
 intracellular free  $\text{Ca}^{2+}$  levels, relationship to heat shock-induced protein synthesis and cytoskeletal rearrangements (*Drosophila melanogaster*), **113**, 402
- Seminiferous epithelium  
 spermatogonia  
 depletion after X irradiation (rhesus monkey), **113**, 473  
 repopulation after X irradiation (rhesus monkey), **113**, 487
- Sensitization  
 to hyperthermia, role of low intracellular pH (CHO cells), **114**, 154
- Serum  
 copper levels, evaluation as index of lung injury after hemithorax exposure to  $\gamma$  rays (rat), **114**, 613  
 mitogenic response of CHO HA-1 cells after hyperthermic cell killing, **113**, 501  
 starvation, and hyperthermic cell killing, effect on viability of CHO HA-1 cells, **113**, 513
- Simian virus 40  
 $\gamma$ -irradiated intranuclear DNA, strand breaks, intracellular induction and repair, analysis (CC91, CV-1 cells), **116**, 462
- Skin  
 collagen biosynthesis,  $\gamma$ -ray-induced increases, 48-week study (mouse), **116**, 145  
 healing wounds, physical strength, effect of X irradiation (mouse), **116**, 135  
 tetrachlorodecaoxide effects after whole-body  $\gamma$  irradiation (rat), **115**, 115  
 tumor induction after repeated  $\beta$  irradiation in limited dose range, 100% incidence (mouse), **115**, 488
- Sodium butyrate  
 effect on  
 CHO HA-1 cell survival after X irradiation, **114**, 186  
 oxygen enhancement ratio of colon tumor cells (human), **113**, 191  
 radiosensitivity and glutathione content of colon tumor cells (human), **114**, 579
- Sonolysis  
 aqueous solutions of pyrimidine derivatives, spin-trapping study, **116**, 56
- Spectroscopy  
 NMR, central nervous system after heavy ion irradiation (rat), **113**, 79
- Spermatogonia  
 in seminiferous epithelium  
 effect of X irradiation (rhesus monkey), **113**, 473  
 repopulation after X irradiation (rhesus monkey), **113**, 487
- SR-4077  
 radiosensitization, thiol oxidation, and inhibition of DNA repair (CHO cells), **113**, 346;  
*erratum*, **114**, 643
- Stem cells  
 hematopoietic, leukotriene-induced radioprotection (mouse), **113**, 388  
 hemopoietic and stromal, recovery in bone marrow after  $\gamma$  irradiation, effect of low dose rate (mouse), **115**, 481
- Sublethal damage  
 and potentially lethal damage  
 in L5178Y lymphoma cells differing in radiation sensitivity (mouse), **113**, 183  
 in L5178Y-R and L5178Y-S cells, effects of reduced temperature and starvation conditions, **113**, 458  
 repair in  $\gamma$ -irradiated normal and malignant cells, *in vitro* analysis (human), **114**, 415
- Sulfate radicals  
 oxidation of methylated uracils: production of radicals, pulse radiolytic analysis, **114**, 207

## Survival

AA8 cells and radiosensitive clones after  $\gamma$  irradiation, **115**, 223

## CHO HA-1 cells

during serum starvation and hyperthermic cell killing, assessment, **113**, 513

after X irradiation, effects of sodium butyrate and 3-aminobenzamide, **114**, 186

L5178Y-R and L5178Y-S cells after X irradiation, relationship to

DNA and chromosome repair (mouse), **115**, 566

initial DNA and chromosome damage (mouse), **115**, 550

V79 cells after acute exposures, effects of multiple small far- or mid-uv light exposures, **114**, 248

## Survival curve

exponential or shouldered, resulting from repair of DNA double-strand breaks, dependence on postirradiation conditions (yeast), **114**, 54

fibroblasts in exponential growth phase, correlation with potentially lethal damage repair capacity, analysis (human), **116**, 74

initial part, evaluation as predictor of fractionated radiotherapy outcome (human), **114**, 425

## T

## Temperature

body, *see* Body temperature

dependence of cytotoxic and radiosensitizing effects of *cis*-dichlorodiammineplatinum(II) on cervical carcinoma cells *in vitro* (human), **114**, 489

## Tetrachlorodecaoxide

regenerative effects after whole-body  $\gamma$  irradiation (rat), **115**, 115

## Therapeutic gain factors

for fractionated irradiation of spontaneous tumors with fast neutrons, photons plus O<sub>2</sub>1 or 3 ATA, or photons plus misonidazole (mouse), **116**, 482

## Thermoresistance

Chinese hamster lung and Morris hepatoma cells, role of hyperthermia-induced Ca<sup>2+</sup>-dependent cellular responses, **113**, 426

## Thermosensitivity

and mitochondrial glutathione depletion, relationship (CHO cells), **115**, 461

## Thermotolerance

defective mutants, isolation and characterization (CHO cells), **113**, 526

development in CHO cells

heated at 45°C at pH 6.6, **115**, 106

after microinjection with glutathione disulfide, **115**, 202

preirradiated intestine, effect on time-temperature relationships (mouse), **113**, 375

role of poly(ADP-ribose)synthetase (V79 cells), **116**, 442

## Thiobutabarbital

effect on tumor blood flow (rat), **114**, 64

## Thiols

low-molecular-weight, interaction with DNA: evidence for counterion condensation and coion depletion near DNA, **114**, 3

net charge and radioprotection of DNA, relationship, **114**, 11

## Thresholds

in radiation exposure responses, guest editorial, **114**, 1

## Thymine glycol

effect on pyrimidine salvage and thymineless radiosensitization in *Escherichia coli thyA* cells, **115**, 617

## Thymine radicals

abstraction of H atom from sugar moiety in oligo- and polydeoxynucleotides, analysis, **116**, 210

## Thymus

microwave irradiation, effect on cellular functional state (rabbit), **115**, 44

nonlymphoid components, effects of  $\gamma$  irradiation *in vitro* (dog), **115**, 84

stromal compartment, effects of graded doses of whole-body neutron and X irradiation (mouse), **113**, 25

## Track structures

high-LET particles, linear simulations: frequency distributions and density functions of distances, **113**, 437

0.3–20-MeV protons, obtained by computer simulations, microdosimetric aspects, **115**, 389

## Transformation

oncogenic, fibroblasts by fractionated doses of neutrons, analysis (mouse), **114**, 589; *erratum*, **116**, 550

## Transplants

bone marrow, role in treatment of victims of nuclear accidents, **113**, 205

## Transport codes

galactic cosmic-ray, analytic benchmark solution, **114**, 201

## Transposons

induced chromosome damage, interaction with X-ray-induced damage: translocations and

- transmission distortion (*Drosophila melanogaster*), **115**, 503
- Tumor bed effect
- associated tissue repair and repopulation, analysis (mouse), **114**, 621
  - induced environmental stress, associated cell subpopulation exclusion within heterogeneous neoplasms: mathematical models, **115**, 533
- Tumor cells, *see also* Cell lines
- brain, sister chromatid exchange, additive induction by X rays and 1,3-bis(2-chloroethyl)-1-nitrosourea (rat), **115**, 187
  - cerebral gliosarcoma, grown as monolayers and spheroids, repair of potentially lethal damage and reentry into cycling phase after X irradiation, comparison (rat), **114**, 515
  - cervical carcinoma
    - with differing radiosensitivity, DNA double-strand breaks, induction and rejoining after  $\gamma$  irradiation (human), **116**, 526
    - oxygen- and temperature-dependent cytotoxic and radiosensitizing effects of *cis*-dichlorodiammineplatinum(II) *in vitro* (human), **114**, 489
  - colon
    - oxygen enhancement ratio, effects of *N*-methylformamide and sodium butyrate (human), **113**, 191
    - radiosensitivity
      - effects of  $\alpha$ -difluoromethylornithine-induced polyamine depletion (human), **114**, 634
      - and glutathione content, changes after exposure to sodium butyrate (human), **114**, 579
  - DS-carcinoma, blood flow, effects of inhalational or injectable anesthetics and of neuroleptic, neuroleptanalgesic, and sedative agents (rat), **114**, 64
  - epithelial teratocarcinoma, radiobiological characterization, DNA damage, and comparison with other rodent and human cell lines, **113**, 278
  - fibrosarcoma
    - changes in bromodeoxyuridine labeling index during radiation treatment (mouse), **116**, 453
    - energy metabolism, effects of pentobarbital anesthesia, analysis by *in vivo*  $^{31}\text{P}$  NMR spectroscopy (mouse), **115**, 361
    - inoculation into  $\gamma$ -irradiated hind thigh: tissue repair and repopulation in tumor bed effect (mouse), **114**, 621
    - late recurrences, radiosensitivity after radiotherapy (mouse), **113**, 334
    - oxygen uptake, inhibition by lonidamine (mouse), **113**, 356
    - proliferation kinetics during fractionated ionizing irradiation (mouse), **116**, 327
    - radiocurability, effect of *N*-methylformamide (mouse), **113**, 199
  - glioma, mass blood flow changes after cerebral  $\gamma$  irradiation (rat), **115**, 586
  - heterogeneous, tumor bed effect-induced environmental stress, associated cell subpopulation exclusion: mathematical models, **115**, 533
  - leukemia, mutation induction by very low dose rate  $\gamma$  irradiation (mouse), **115**, 273
  - Lewis lung carcinoma, blood flow reduction by hydralazine after X irradiation, effect on efficacy of misonidazole and RSU-1069 (mouse), **115**, 292
  - lymphoma, strains differing in radiation sensitivity, repair of potentially lethal damage and sublethal damage (mouse), **113**, 183
  - mammary
    - cell cycle effect on X-ray-induced DNA double- and single-strand breaks, comparison (mouse), **116**, 228
    - EMT6, response to X irradiation, effects of porfiromycin (mouse), **116**, 100
    - energy metabolism, effects of pentobarbital anesthesia, analysis by *in vivo*  $^{31}\text{P}$  NMR spectroscopy (mouse), **115**, 361
    - radiocurability, effect of *N*-methylformamide (mouse), **113**, 199
    - toxic effects of acute glutathione depletion by L-buthionine sulfoximine and dimethylfumurate (mouse), **114**, 215
  - melanoma
    - delay in initiation of DNA synthesis after irradiation, effect of oxygen (mouse), **113**, 102
    - lung metastases and lysis by natural killer cells, comparative effects of daily and weekly fractions of X irradiation (mouse), **114**, 354
  - Morris hepatoma, thermoresistance, role of hyperthermia-induced  $\text{Ca}^{2+}$ -dependent cellular responses, **113**, 426
  - neuroblastoma, synchronized, proliferation after heat treatment, role of heat-shock proteins (mouse), **113**, 252
  - ovarian, induction in BC3F<sub>1</sub> mouse after low dose neutron and X irradiation, **113**, 362
  - pheochromocytoma, intracellular  $\text{Ca}^{2+}$  levels and inositol lipid metabolism, effects of hyperthermia (rat), **113**, 414

- pulmonary, DNA strand breaks and 1- $\beta$ -D-arabino-furanosylcytosine-detectable sites induced by X and  $\gamma$  irradiation, comparison (human), **114**, 168
- radiosensitivity, chemosensitivity, and inherent factors, assessment techniques, implications for clinical oncology (human), **114**, 401
- rhabdomyosarcoma, radiosensitization *in vivo* by diethylthiocarbamate (mouse), **116**, 539
- RIF-1
- killing with 8-hydroxyquinoline, evaluation (mouse), **115**, 373
  - treatment with etomidate and Gibbs clip, evaluation (mouse), **114**, 105
- skin, induction after repeated  $\beta$  irradiation in limited dose range, 100% incidence (mouse), **115**, 488
- survival curve, initial part, evaluation as predictor of fractionated radiotherapy outcome (human), **114**, 425
- various types
- fractionated irradiation with fast neutrons, photons plus O<sub>2</sub>1 or 3 ATA, or photons plus misonidazole, therapeutic gain factors (mouse), **116**, 482
  - radiosensitivity, enhancement by postirradiation hypoxia: time course and oxygen concentration dependency (human, mouse), **116**, 124
  - response to  $\gamma$  irradiation, *in vitro* analysis (human), **114**, 415

## U

## Ultraviolet irradiation

- DNA
- subsequent cleavage by *Micrococcus luteus*  $\gamma$ -endonuclease, analysis, **114**, 556
  - wavelength dependence of redoxo-endonuclease-mediated cleavage at photoproduct formation sites (human), **113**, 543
- fibroblasts at solar wavelengths, induction of DNA single-strand breaks, analysis (human skin), **116**, 313
- proadipocytes, induced DNA damage, effect of cellular differentiation on repair (mouse), **116**, 217
- V79 cells, sensitivity to acute exposures, alteration by multiple small far- or mid-uv light exposures, measurement by cell lethality and mutagenesis, **114**, 248
- wild-type eukaryotes and *Escherichia coli*, comparative action spectra (254–320 nm), **114**, 307

- and X irradiation, quantitative aspects of interactive killing effects in bacteria, **115**, 124
- Uracils
- methylated, radicals produced via SO<sub>4</sub><sup>-</sup> oxidation, pulse radiolytic analysis, **114**, 207
- Urethan
- effect on tumor blood flow (rat), **114**, 64

## V

## V79 cells

- $\gamma$ -ray- and fission-spectrum neutron-induced chromosome damage, radioprotective effects of WR-1065, **113**, 145
- radiobiological characterization, DNA damage, and comparison with human epithelial teratocarcinoma cells, **113**, 278
- radiosensitivity

  - and DNA double-strand break repair, comparison, **113**, 268
  - enhancement by postirradiation hypoxia: time course and oxygen concentration dependency, **116**, 124
  - repair of radiation-induced chromatin damage, effects of glutathione depletion and hypoxia, **116**, 89
  - sensitivity to *N*-methyl-*N*'-nitro-*N*-nitrosoguanidine, effect of  $\gamma$  preirradiation, **115**, 609
  - sequential exposures to high- and low-LET radiations: damage interaction effects as function of cell cycle stage, **115**, 54
  - thermotolerance and radiation and heat responses, role of poly(ADP-ribose)synthetase, **116**, 442
  - treated with hypertonic phosphate-buffered saline after  $\gamma$  or X irradiation, interaction function  $\gamma(x)$  estimation, **116**, 472

- X irradiation, lethal effects, modulation by caffeine, **115**, 176
- X-ray-induced DNA double-strand breaks, measurement by neutral filter elution: calibration by <sup>125</sup>I decay, **115**, 624

## W

## Water

- condensed, absolute scattering probabilities for subexcitation electrons, determination, **114**, 467
- electron-pulsed ice, red luminescence emission, **115**, 403

## Wavelength

- uv irradiation, role in redoxo-endonuclease-mediated DNA cleavage at photoproduct formation sites (human), **113**, 543

- Wound healing  
 skin, effect of X irradiation (mouse), **116**, 135
- WR-1065  
 oxidation, influencing factors, **113**, 243  
 radioprotective effects on  
 $\gamma$ -ray- and fission-spectrum neutron-induced chromosome damage (V79 cells), **113**, 145  
 $\gamma$ -ray-induced DNA single-strand breaks in CHO cells, **113**, 155  
 jejunum, *in vivo* effects on DNA strand break induction and rejoining (mouse), **114**, 268  
 and WR-2721, opposite effects on  $\gamma$ -ray-induced hypothermia, correlation with oxygen uptake (guinea pig), **114**, 240
- WR-2721  
 and/or 16,16-dimethylprostaglandin E<sub>2</sub>, radioprotection against fission neutron- $\gamma$  irradiation (mouse), **115**, 605  
 effects on X-ray-induced changes in collagen isotypes I, III, and IV (murine lung), **115**, 515  
 entry into brain across modified blood-brain barrier (rat), **115**, 303  
 radioprotection of jejunum, *in vivo* effects on DNA strand break induction and rejoining (mouse), **114**, 268  
 and WR-1065, opposite effects on  $\gamma$ -ray-induced hypothermia: correlation with oxygen uptake, analysis (guinea pig), **114**, 240
- X
- X irradiation  
 L- $\alpha$ -amino-*n*-butyric acid HCl containing 1.5% L-cysteine HCl, ESR study of generated radicals, **116**, 373  
 BC3F<sub>1</sub> mouse at low dosage, tumor induction and life-shortening, **113**, 362
- brain  
 induced alterations of neuronal chromatic structure in cerebellum, analysis (rat), **114**, 94  
 tumor cells, and treatment with 1,3-bis(2-chloroethyl)-1-nitrosourea, additive induction of sister chromatid exchange (rat), **115**, 187
- cerebral gliosarcoma cells grown as monolayers and spheroids, subsequent repair of potentially lethal damage and reentry into cycling phase, comparison (rat), **114**, 515
- cervical carcinoma cells *in vitro*: oxygen- and temperature-dependent cytotoxic and radiosensitizing effects of *cis*-dichlorodiammineplatinum(II) (human), **114**, 489
- CHO cells  
 HA-1, subsequent survival, effects of sodium butyrate and 3-aminobenzamide (Chinese hamster), **114**, 186  
 induced G<sub>2</sub> arrest, effects of poly(adenosinediphosphoribose) synthesis inhibitors and structurally related compounds, **113**, 58  
 sensitivity, effect of dimethylfumarate, **115**, 495
- CHO-tsH1 and CHO-SC1 cells, protein synthesis and split-dose recovery, **114**, 281
- colon tumor cells  
 changes in radiosensitivity after exposure to sodium butyrate (human), **114**, 579  
 oxygen enhancement ratio, effects of *N*-methylformamide and sodium butyrate (human), **113**, 191
- dose fractionation, sensitivity of hepatocyte clonogens (mouse), **113**, 51
- Drosophila melanogaster*, induced chromosome damage, interaction with transposon-induced damage: translocations and transmission distortion, **115**, 503
- epithelial teratocarcinoma cells, DNA damage and survival parameters, comparison with V79 cells (human), **113**, 278
- guanine hydrochloride monohydrate single crystals, formation of secondary radicals, reaction mechanisms, ESR and ENDOR spectroscopy, **116**, 379
- guanosine 5'-monophosphate single crystals at 10° K, ESR/ENDOR study, **116**, 196
- hepatocytes, long-term repair *in vivo* of colony-forming ability and chromosomal injury, analysis (mouse), **113**, 40
- Hodgkin's disease patient, induction of structural chromosome aberrations in peripheral lymphocytes, **114**, 528
- human cell lines, induction of DNA strand breaks and 1- $\beta$ -D-arabinofuranosylcytosine detectable sites, **114**, 168
- intestine, and hyperthermia, induction of thermotolerance, effect on time-temperature relationships (mouse), **113**, 375
- kidney, response to very small doses per fraction, comparison to neutron irradiation (mouse), **114**, 385
- lens epithelial cells, sensitivity to induction of growth arrest after stimulation from quiescence (rat), **113**, 133
- Lewis lung carcinoma, subsequent blood flow reduction by hydralazine, effect on efficacy of misonidazole and RSU-1069 (mouse), **115**, 292

- limb, induced carcinogenesis, effect of hyperthermia (mouse), **115**, 448
- lung, changes in collagen isotypes I, III, and IV, effects of time, dose, and WR-2721 (mouse), **115**, 515
- L5178Y lymphoma cell strains differing in radiation sensitivity, repair of potentially lethal damage and sublethal damage (mouse), **113**, 183
- L5178Y-R and L5178Y-S cells, difference in radiosensitivity, role of  
DNA and chromosome repair (mouse), **115**, 566  
initial DNA and chromosome damage (mouse), **115**, 550
- mammary tumor cells  
effects of porfiromycin (mouse), **116**, 100  
induced DNA double- and single-strand breaks, cell cycle effects, comparison (mouse), **116**, 228
- mice  
effect on physical strength of healing skin wounds, **116**, 135  
inoculated with B16<sub>a</sub> melanoma, effects of daily and weekly fractions on lung metastases and natural killer cell activity, **114**, 354  
and neutron irradiation, lens epithelial cells, recovery from single and fractionated doses, comparison (mouse), **114**, 567  
normal hamster cells, mouse cells, and transformed mouse cells, repair of potentially lethal damage, inhibition by hyperthermia, **113**, 171  
plateau-phase CHO cells, induced chromosome damage, effect of arabinofuranosyladenine: implications for repair and fixation of  $\alpha$ -potentially lethal damage, **114**, 361  
preimplantation embryos, induction of nonlethal changes, assay with embryo aggregation chimeras (mouse), **113**, 289  
prenatal, effects on appearance of reflexes and physiological markers (rat), **116**, 416  
rhabdomyosarcoma *in vivo*, radiosensitization by diethylthiocarbamate (mouse), **116**, 539  
RIF-1 tumors, combined with 8-hydroxyquinoline treatment, in tumor-targeted cell killing, evaluation (mouse), **115**, 373  
semiferous epithelium  
depletion of spermatogonia (rhesus monkey), **113**, 473  
subsequent repopulation of spermatogonia (rhesus monkey), **113**, 487  
total lymphoid, late somatic effects (mouse), **116**, 503  
tumor cells, radiosensitivity enhancement by postirradiation hypoxia: time course and oxygen concentration dependency (hamster, human, mouse), **116**, 124  
and uv irradiation or nitrogen mustard treatment, quantitative aspects of interactive killing effects in bacteria, **115**, 124
- V79 cells  
combination with exposure to argon and neon ions: damage interaction effects as function of cell cycle stage, **115**, 54  
induced DNA double-strand breaks, measurement by neutral filter elution: calibration by <sup>125</sup>I decay, **115**, 624  
induced potentially lethal damage, repair, metabolic effects of cordycepin and 2-halo derivatives, **114**, 231  
lethal effects, modulation by caffeine, **115**, 176  
and treatment with hypertonic phosphate-buffered saline: estimation of interaction function  $\gamma(x)$ , **116**, 472  
whole-body, effect of graded doses on stromal compartment of thymus (mouse), **113**, 25
- Xeroderma pigmentosum  
fibroblasts from patients, and normal fibroblasts, DNA, proximity of repair patches to persistent pyrimidine dimers, analysis, **116**, 245
- Xylazine  
with ketamine, effect on tumor blood flow (rat), **114**, 64
- $\gamma$
- Yeast  
mutant *rad54-3*, repair of DNA double-strand breaks, resultant exponential or shouldered survival curves, dependence on postirradiation conditions, **114**, 54  
*Saccharomyces cerevisiae*, diploid strain, mitotic recombination after continuous long-term  $\gamma$  irradiation, **113**, 71
- Z
- Zacopride  
effects on  $\gamma$  radiation-induced emesis (rhesus monkey), **115**, 595